เอทานอลดีไฮเดรชันบนตัวเร่งปฏิกิริยาวัสดุเชิงประกอบอะลูมินา-อนุภาคซิลิกาทรงกลมที่ได้จากวิธีโซลเจลที่ปรับปรุง

นายไพโรจน์ โตแฉ่ง

วิทยานิพนธ์นี้เป็นส่วนหนึ่งของการศึกษาตามหลักสูตรปริญญาวิศวกรรมศาสตรมหาบัณฑิต
สาขาวิชาวิศวกรรมเคมี ภาควิชาวิศวกรรมเคมี
คณะวิศวกรรมศาสตร์ จุฬาลงกรณ์มหาวิทยาลัย
ปีการศึกษา 2559

THE ETHANOL DEHYDRATION OVER ALUMINA-SPHERICAL SILICA PARTICLE COMPOSITE CATALYST FROM MODIFIED SOL-GEL METHOD

Mr. Phairoj Tochaeng

A Thesis Submitted in Partial Fulfillment of the Requirements
for the Degree of Master of Engineering Program in Chemical Engineering
Department of Chemical Engineering
Faculty of Engineering
Chulalongkorn University
Academic Year 2016

Thesis Title	THE ETHANOL DEHYDRATION OVER ALUMINA-SPHERICAL SILICA PARTICLE COMPOSITE CATALYST FROM MODIFIED SOL-GEL METHOD
By	Mr. Phairoj Tochaeng
Field of Study	Chemical Engineering
Thesis Advisor	Professor Bunjerd Jongsomjit, Ph.D.

Accepted by the Faculty of Engineering, Chulalongkorn University in Partial Fulfillment of the Requirements for the Master's Degree

.....Dean of the Faculty of Engineering
(Associate Professor Supot Teachavorasinskun, D.Eng.)

THESIS COMMITTEE

.....Chairman
(Associate Professor Muenduen Phisalaphong, Ph.D.)

.....Thesis Advisor
(Professor Bunjerd Jongsomjit, Ph.D.)

.....Examiner
(Chutimon Satirapipathkul, D.Eng.)

.....External Examiner
(Ekrachan Chaichana, D.Eng.)

ไพโรจน์ โตแฉ่ง : เอทานอลดีไฮเดรชันบนตัวเร่งปฏิกิริยาวัสดุเชิงประกอบอะลูมินา-อนุภาคซิลิกาทรงกลมที่ได้จากวิธีโซลเจลที่ปรับปรุง (THE ETHANOL DEHYDRATION OVER ALUMINA-SPHERICAL SILICA PARTICLE COMPOSITE CATALYST FROM MODIFIED SOL-GEL METHOD) อ.ที่ปรึกษาวิทยานิพนธ์หลัก: ศ. ดร. บรรเจิด จงสมจิตร, 86 หน้า.

ตัวเร่งปฏิกิริยาอนุภาคซิลิกาทรงกลมและตัวเร่งปฏิกิริยาวัสดุเชิงประกอบอะลูมินา-อนุภาคซิลิกาทรงกลมถูกทดสอบสำหรับคุณสมบัติทางการเร่งปฏิกิริยา และความว่องไวในการเร่งปฏิกิริยาโดยผ่านปฏิกิริยาขจัดน้ำของเอทานอล ตัวเร่งปฏิกิริยาอนุภาคซิลิกาทรงกลมและตัวเร่งปฏิกิริยาวัสดุเชิงประกอบอะลูมินา-อนุภาคซิลิกาทรงกลมถูกเตรียมโดยวิธีโซลเจลที่ปรับปรุงด้วยการเปลี่ยนปริมาณของอะลูมินาในช่วงตั้งแต่ 20 ถึง 80 โมลเปอร์เซ็นต์ คุณสมบัติของตัวเร่งปฏิกิริยาเหล่านี้ถูกพิสูจน์โดยการวิเคราะห์การสลายตัวของสารเมื่อได้รับความร้อน การส่องกราดด้วยกล้องจุลทรรศน์อิเล็กตรอน การกระเจิงรังสีเอ็กซ์ การวิเคราะห์สารด้วยรังสีอินฟราเรด การกระจายตัวธาตุด้วยรังสีเอ็กซ์ การหาปริมาณสารด้วยรังสีเอ็กซ์ฟูออเรสเซนต์ การคายแอมโมเนียด้วยการเพิ่มอุณหภูมิแบบตั้งโปรแกรม และ การดูดซับทางกายภาพด้วยไนโตรเจน ในส่วนแรก ปฏิกิริยาขจัดน้ำของเอทานอลในสถานะแก๊สตัวเร่งปฏิกิริยาวัสดุเชิงประกอบอะลูมินา-อนุภาคซิลิกาทรงกลมถูกดำเนินการในเครื่องปฏิกรณ์เคมีแบบเบดคงที่ ที่ความดันบรรยากาศด้วยอุณหภูมิค่าต่าง ๆ จาก 200 ถึง 400 องศาเซลเซียส ตัวเร่งปฏิกิริยาวัสดุเชิงประกอบร้อยละ 60 โดยโมลของอะลูมินาบน ซิลิกา หรือ 60Al-SSP แสดงความเป็นกรดที่สูงกว่าตัวอื่นๆ การเปลี่ยนแปลงเอทานอลและการเลือกเกิด ขึ้นอยู่กับปริมาณอะลูมินาและอุณหภูมิของปฏิกิริยา ที่อุณหภูมิต่ำ ไดเอทิลอีเทอร์ถูกผลิตขึ้นมาในปริมาณที่มีนัยสำคัญ ในขณะที่อุณหภูมิสูง เอทิลีนเป็นผลิตภัณฑ์หลัก พบว่าตัวเร่งปฏิกิริยาวัสดุเชิงประกอบ 60Al-SSP แสดงการเปลี่ยนแปลงเอทานอลและการเลือกเกิดเอทิลีนมากที่สุด การทดลองในส่วนต่อไป พบว่าการเพิ่มปริมาณน้ำในสารตั้งต้น นำไปสู่การเพิ่มขึ้นของการเปลี่ยนแปลงเอทานอลและการเลือกเกิดเป็นเอทิลีนที่อุณหภูมิสูง แต่ค่าก็ยังต่ำกว่าการใช้เอทานอลบริสุทธิ์ ในส่วนสุดท้าย ประสิทธิภาพของตัวเร่งปฏิกิริยาวัสดุเชิงประกอบ 60Al-SSP โดยการทดสอบผ่านเวลาที่ใช้ในการดำเนินการปฏิกิริยาที่ 10 ชั่วโมงถูกตรวจสอบ ผลการทดลองแสดงให้เห็นว่าการเปลี่ยนแปลงเอทานอลและการเลือกเกิดเอทิลีนของเอทานอลบริสุทธิ์จะรักษาไว้ที่ค่าที่สูงในระหว่าง 10 ชั่วโมง ในขณะที่ การเปลี่ยนแปลงเอทานอลและการเลือกเกิดเอทิลีนของเอทานอลชีวภาพจะเพิ่มอย่างช้า ๆ และการเกิดถ่านบนตัวเร่งปฏิกิริยาวัสดุเชิงประกอบ 60Al-SSP ที่ใช้เอทานอลบริสุทธิ์จะสูงกว่าเอทานอลชีวภาพ

ภาควิชา วิศวกรรมเคมี ลายมือชื่อนิสิต .....

สาขาวิชา วิศวกรรมเคมี ลายมือชื่อ อ.ที่ปรึกษาหลัก .....

ปีการศึกษา 2559

5670529121 : MAJOR CHEMICAL ENGINEERING
KEYWORDS: ALUMINA-SILICA COMPOSITE CATALYSTS / SOLID ACID CATALYSTS / ETHANOL DEHYDRATION / ETHYLENE / BIOETHANOL

PHAIROJ TOCHAENG: THE ETHANOL DEHYDRATION OVER ALUMINA-SPHERICAL SILICA PARTICLE COMPOSITE CATALYST FROM MODIFIED SOL-GEL METHOD. ADVISOR: PROF. BUNJERD JONGSOMJIT, Ph.D., 86 pp.

The spherical silica particle (SSP) and alumina silica composite (Al-SSP) catalysts were investigated for catalytic properties and catalytic activity via dehydration of ethanol. The SSP and Al-SSP catalysts were prepared by modified sol gel method with various alumina content ranges from 20 to 80 mol%. The properties of these catalysts were characterized by TGA, SEM, XRD, FTIR, EDX, XRF, NH_3-TPD and nitrogen physisorption. In the first part, the dehydration of ethanol in gas phase over SSP and Al-SSP catalysts was performed in a fix-bed reactor at the atmospheric pressure with various temperatures from 200 to 400 ºC. The 60Al-SSP catalyst exhibited significantly higher acidity than the others. The ethanol conversion and selectivity depend on alumina content and reaction temperature. At lower temperature, diethyl ether was produced in significant quantities, while at higher temperature, ethylene was the major product. It was found that the 60Al-SSP exhibited the highest ethanol conversion and ethylene selectivity. The next part, it was found that the increasing of water content in reactant led to the increasing of ethanol conversion and ethylene yield at high temperature. However, it remains below the ethanol conversion and ethylene yield of pure ethanol. In the last part, the performance of 60Al-SSP via time on stream (TOS) test for 10 hours was investigated. The results showed that the conversion of ethanol and ethylene yield of pure ethanol kept constant at high during 10 hours, while the conversion and the ethylene yield of bioethanol slowly increased. And the coke formation on 60Al-SSP catalyst with using pure ethanol was higher than bioethanol.

Department:	Chemical Engineering	Student's Signature	.....
Field of Study:	Chemical Engineering	Advisor's Signature	.....
Academic Year:	2016		

ACKNOWLEDGEMENTS

I would like to express my sincere thanks to my thesis advisor, Prof. Dr. Bunjerd Jongsomjit for his guidance, counsel, guidelines for solving problem and constant encouragement throughout the course of this study.

Furthermore, I'm thankful to Assoc. Prof. Dr. Muenduen Phisalaphong, as a chairman, Dr. Chutimon Satirapipathkul and Dr. Eakrachan Chaichana as the members of the thesis committee.

Thankful for assistance and imposing suggestion to Dr. Mingkwan Wannaborworn, Dr. Jakrapan Janlamool and each friends in the laboratory who always provision the furtherance thorough this study.

Finally, I would like to thank Chula Uniserch, Chulalongkorn University (CU-56-654-AM) for the financial support of this project.

CONTENTS

Page

Page

Page

Page

LIST OF TABLES

LIST OF FIGURES

CHAPTER I
INTRODUCTION

1.1 General introduction

Ethylene is an important raw material in the petrochemical industry. At present, petrochemical products are produced from ethylene, including ethylene oxide, ethyl benzene, ethylene glycol, acetaldehyde, acetic acid, vinyl chloride, styrene, vinyl acetate, polyethylene, and polyvinyl chloride [1]. In general, ethylene is produced by steam cracking of hydrocarbons. Some products from this process can cause the environmental problem. In addition, the purification process of ethylene is required leading to high investment and operating cost. Therefore, the new beneficial methods of ethylene production process need to be established. Nowadays, the production of ethylene by catalytic ethanol dehydration is used because of its green alternatives for manufacturing ethylene, to reduce greenhouse gas emissions. Moreover, ethanol can be produced from renewable sources, therefore, it does not depend on petroleum source. Two reactions can occur in parallel during catalytic dehydration of ethanol:

$C_2H_5OH \rightarrow C_2H_4 + H_2O$ ΔH_{298} = + 44.9 kJ/mol (1)

$2C_2H_5OH \rightarrow C_2H_5OC_2H_5 + H_2O$ ΔH_{298} = - 25.1 kJ/mol (2)

Reactions (1) and (2) are endothermic and exothermic, respectively. The main product is ethylene, whereas diethyl ether (DEE), acetaldehyde and light olefins are byproducts. Each of products is produced at the different temperatures. For example, the high temperature (400 - 450°C) is suitable to produce ethylene, while the byproduct is gained at lower temperature (< 300 °C) [2-4].

Solid catalysts with acidic character were considered to have high activity for ethanol dehydration reaction. It is well known that ethylene formation via dehydration of ethanol is catalyzed by various solid acid catalysts such as titania-silica, magnesium oxides, zeolite, zirconium phosphite, cobalt oxides, and chromium oxides [5].

Alumina is an important catalyst or support in many industrial processes. It has long been found that alumina could be used for the alcohol dehydration reaction and also used in many other chemical reactions such as catalytic cracking, isomerization, and alkylation, etc. The using of alumina in catalyst field provides excellent high degree of metal dispersion, moderate high surface area, and thermal stability over wide range temperature [6, 7]. Silica is often used as support for various transition metals. It possesses high activity in gas-phase and liquid-phase oxidation processes [8]. Spherical silica particle is used in supported catalyst because it has an excellent morphology due to the smoothness of spherical particles [9]. In the study, we used modified sol-gel method to prepare the catalyst. This method improves dispersion of alumina on spherical silica particle surface. Moreover, it is easy to use to prepare mixed oxide catalyst. In fact, the Al-SSP composite is used as a support or catalyst depending on required active site of reaction. This composite catalyst is bi-functional catalysts containing mostly acid sites presented on its surface [10].

1.2 Research objectives

- To determine the activity and selectivity of Al-SSP composite catalysts for the dehydration reaction of ethanol.
- To investigate the effect of ethanol concentration on Al-SSP composite catalysts for the dehydration reaction of ethanol.
- To investigate the stability of Al-SSP composite catalysts for the dehydration reaction of ethanol.

1.3 Research scopes

- Preparation of spherical silica particle (SSP) by sol-gel method.
- Preparation of Al-SSP composite catalysts with 20-80 mol% of alumina on SSP support by modified sol-gel method.
- Characterization of SSP and Al-SSP composite catalysts by nitrogen physisorption , X-ray diffraction (XRD), X-ray fluorescence spectrometry (XRF), scanning electron microscopy (SEM), energy dispersive X-ray spectroscopy (EDX), temperature programed adsorption (NH_3-TPD), Fourier transform infrared spectroscopy (FTIR), thermal gravimetric analysis (TGA).
- Investigation the catalytic performance of SSP and Al-SSP composite catalysts in ethanol dehydration reaction under atmospheric pressure and temperature between 200 ºC to 400 ºC.
- Investigation the effect of ethanol concentration on Al-SSP composite catalysts for the dehydration reaction of ethanol.
- Investigation the stability of all catalysts in ethanol dehydration reaction within time on stream (TOS) around 10 hrs.

1.4 Research methodology

Part I: Characterization and catalytic activity test of alumina-silica composite catalysts.

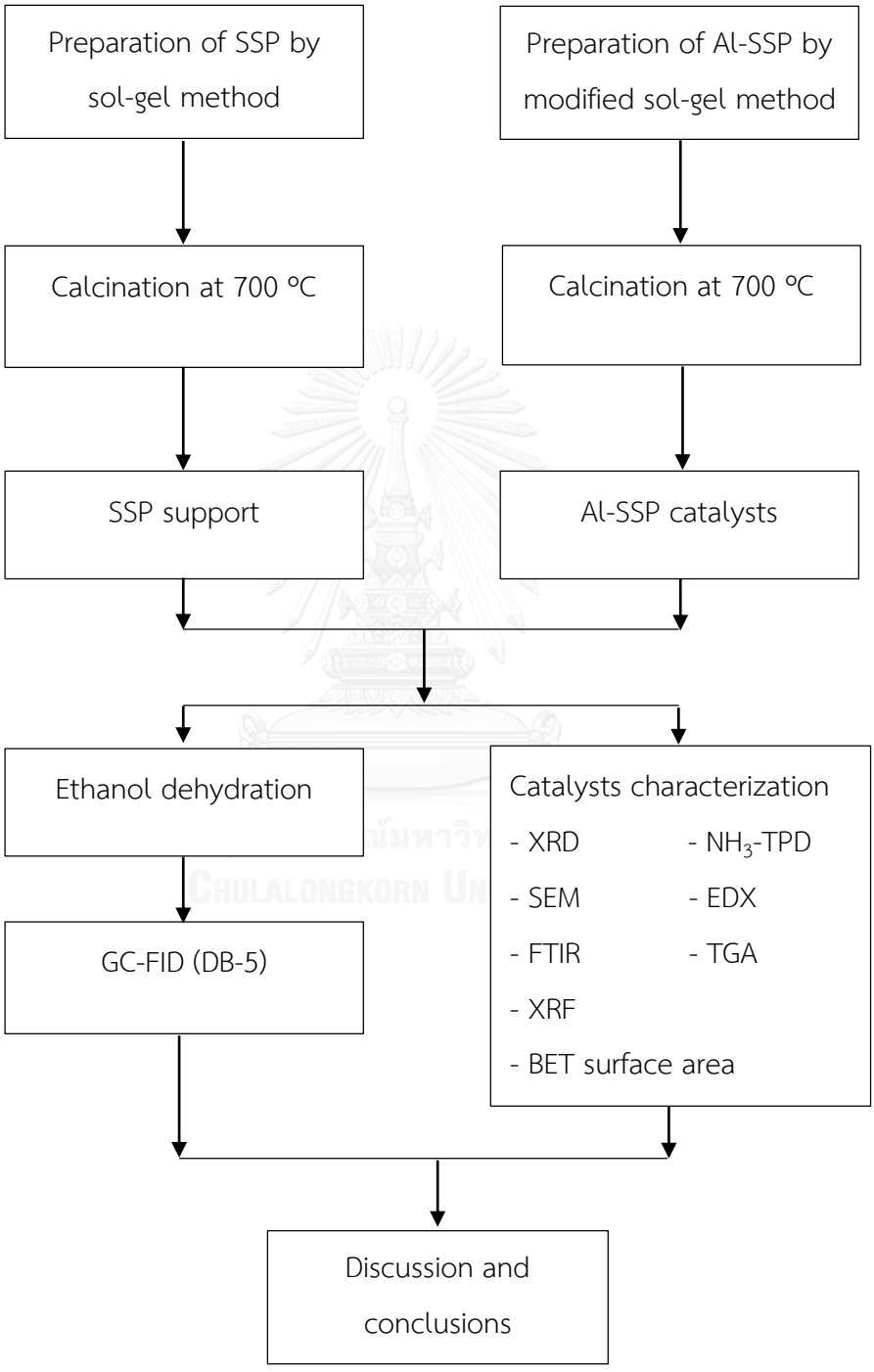

Part II: Investigation catalytic activity of 60Al-SSP in ethanol dehydration reaction with different ethanol concentrations.

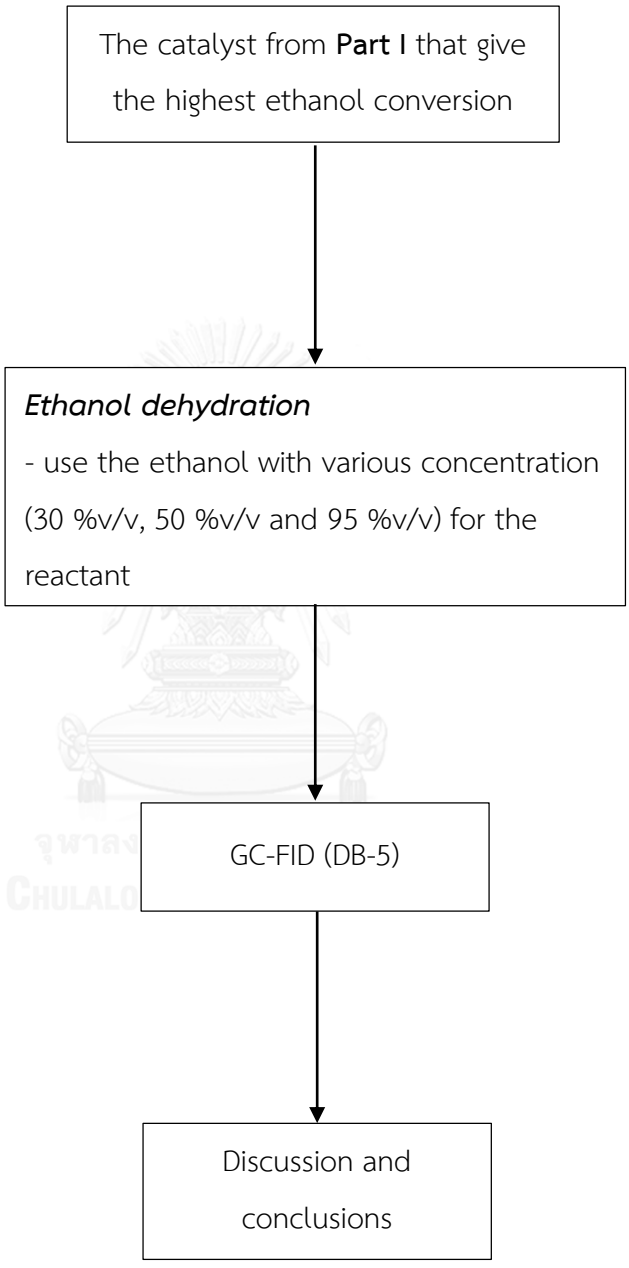

Part III: Investigation of time on stream test of 60Al-SSP in ethanol dehydration.

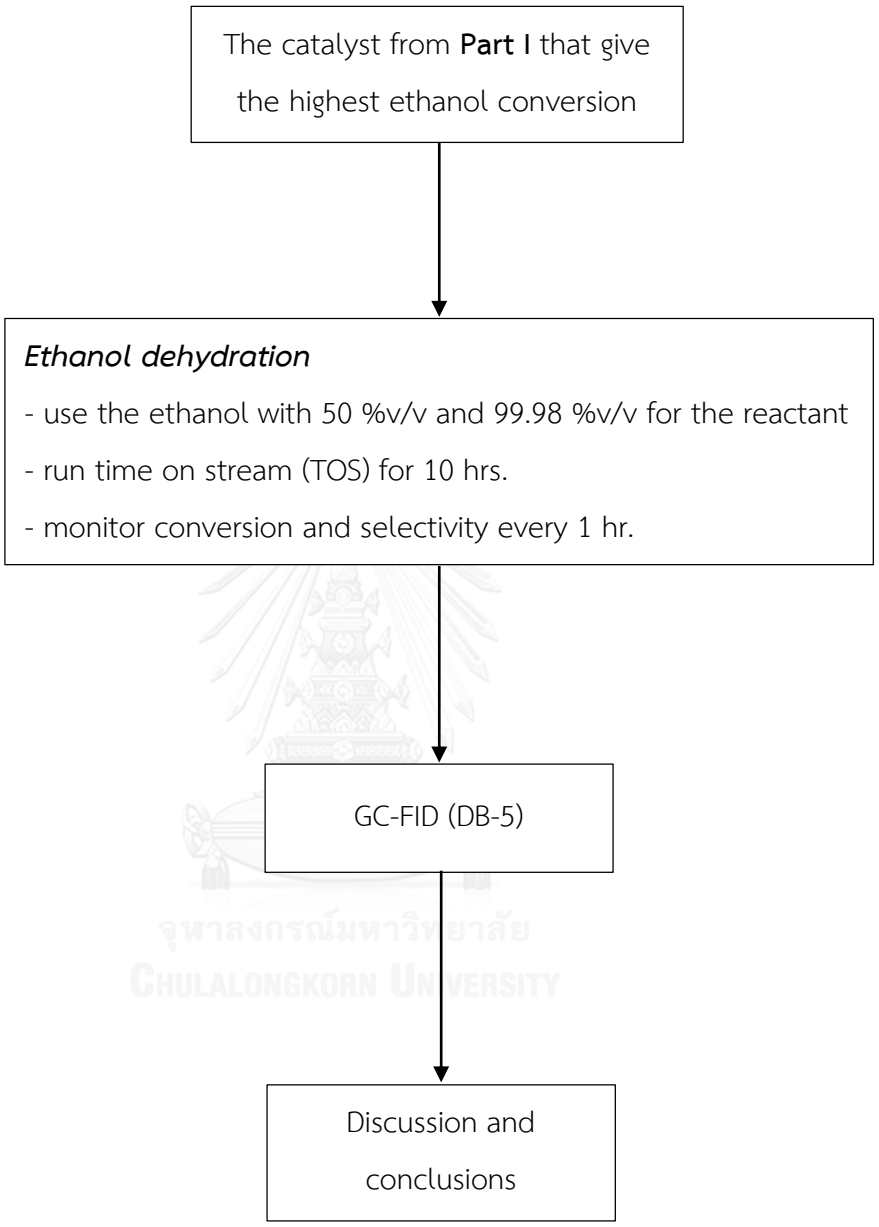

CHAPTER II

THEORY AND LITERATURE REVIEWS

2.1 Ethanol dehydration reaction

2.1.1 Reaction mechanisms for ethanol dehydration

Ethanol dehydration can occur two competitive paths. The intramolecular dehydration of ethanol to ethylene is the important reaction and the other is intermolecular dehydration of ethanol to diethyl ether. At higher temperature, ethylene is the dominant product, while, diethyl ether is produced insignificant quantities at the lower temperature. Moreover, at the higher temperature, the ethanol dehydration to acetaldehyde can occur as a side reaction [1 1] . The ethanol dehydration reaction to generate the ethylene and diethyl ether can be concluded as three kinds of route: (1) parallel reaction, (2) a series of reactions, and (3) a parallel series reaction, is shown in **Figure 2.1** [12].

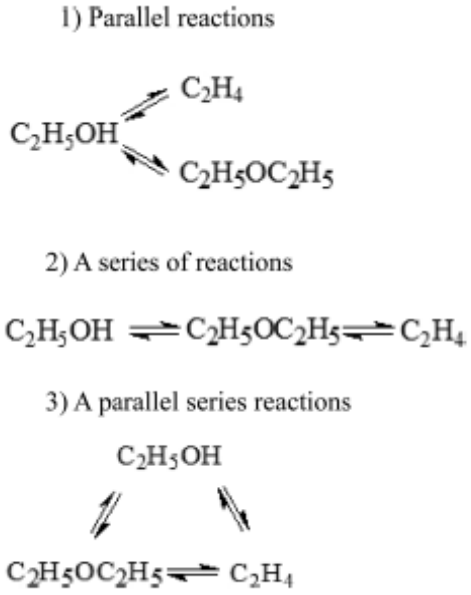

Figure 2.1 Mechanism of dehydration of ethanol [12].

Ethylene from the dehydration of ethanol, the first step, an acid catalyst protonates the hydroxyl group, which leaves as a water molecule. And then, the conjugate base of the catalyst deprotonates the methyl group, and the hydrocarbon rearranges into ethylene. This mechanism as shown in **Figure 2.2.** In this reaction requires strong acid site or Brønsted acid sites and high operating temperature (ranging from 180 °C to 500 °C) [2].

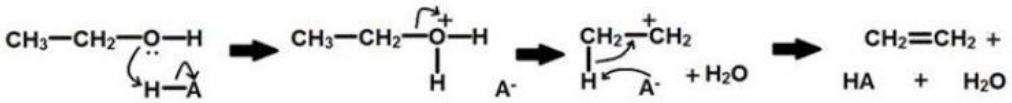

Figure 2.2 Mechanism for dehydration of ethanol to ethylene [2].

The ethanol dehydration to diethyl ether requires weak acid site and low operating temperature (below 240 °C) [1]. The mechanism of ethanol to diethyl ether is substitution reaction. The reaction to generate diethyl ether explains by substitution nucleophilic unimolecular reaction (S_N1) or substitution nucleophilic bimolecular reaction (S_N2).

For the S_N2 reaction, the lone- pair electrons of nucleophiles attack the electrophilic electron deficient central atom creating the intermediate. At the same time, water molecule is lost and rearrangement to diethyl ether. The S_N2 reaction does not create the carbocation. The mechanisms of ethanol to diethyl ether in the S_N1 and S_N2 reaction are shown in **Figure 2.3** and **Figure 2.4**, respectively [13].

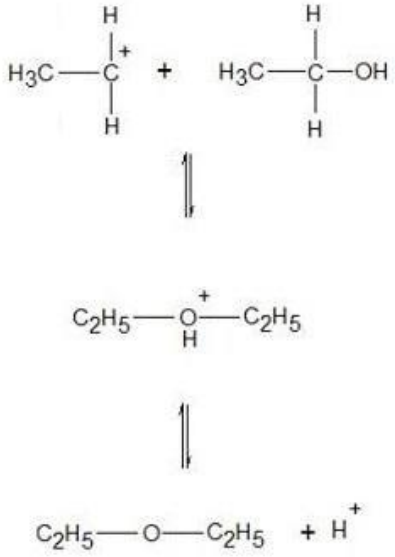

Figure 2.3 The ethanol dehydration mechanism to DEE in the S_N1 reaction [13].

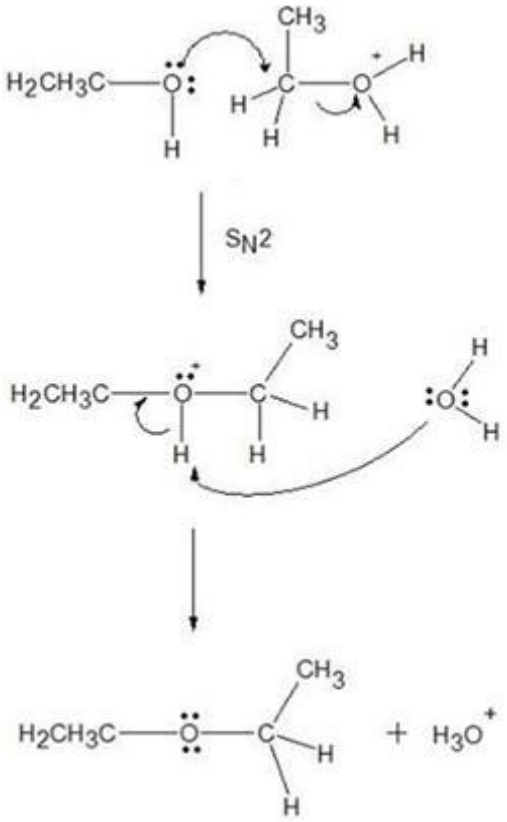

Figure 2.4 The ethanol dehydration mechanism to DEE in the S_N2 reaction [13].

However, other research papers on the dehydration of ethanol to ethylene report that this reaction requires Lewis acid sites, especially for alumina and silica-alumina catalysts [3, 14-16]. The adsorption and reaction mechanisms for ethanol dehydration over Lewis acid catalysts is shown in **Figure 2.5**. The first part, ethanol adsorbs by replacing hydroxyl groups forming ethoxy groups and gas-phase water. Another part of it likely dissociatively adsorbs on Lewis acid-base pairs forming ethoxy groups and new OHs. The surface ethoxy groups are intermediate species for both diethyl ether and ethylene production. The diethyl ether may form by a nucleophilic substitution reaction where ethoxy groups attack as nucleophiles the carbon atom of either gas-phase ethanol, or, more likely, of H-bonded adsorbed undissociated ethanol. This reaction, reversible, disappears in favor of ethoxy group decomposition to ethylene when the concentration of available undissociated ethanol is very low [16].

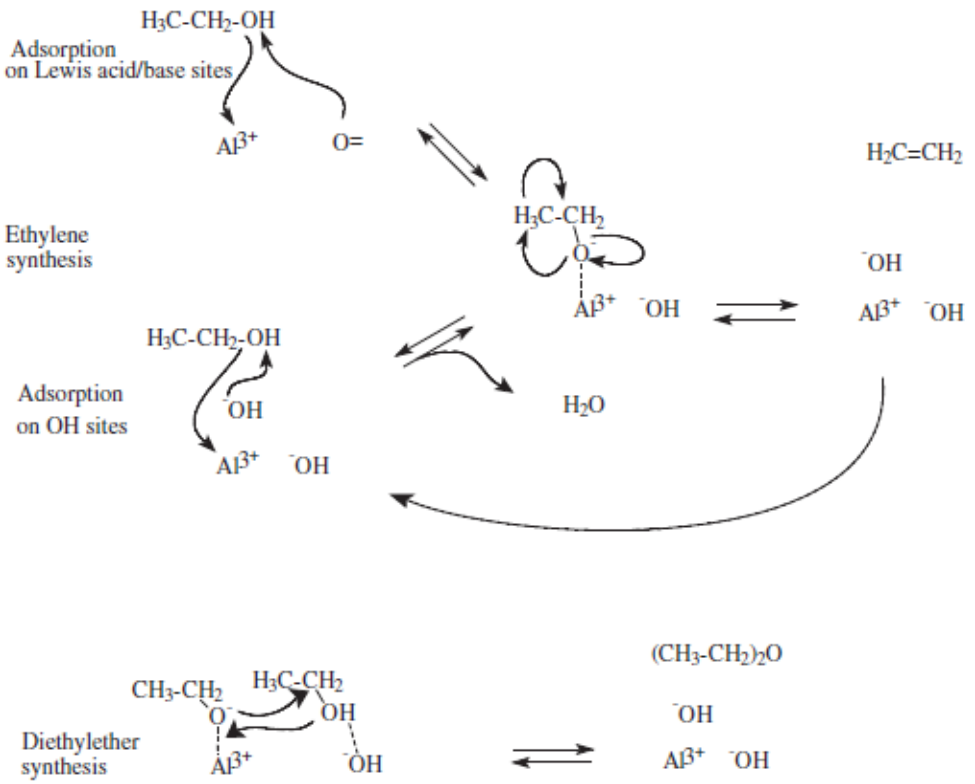

Figure 2.5 The adsorption and reaction mechanisms for ethanol dehydration over Lewis acid catalysts [16].

2.1.2 Effect of water on catalytic performance of alumina and alumina silica catalyst.

Using bioethanol as a reactant, water was shown to have a significant effect on the ethanol dehydration on alumina-based catalyst. **Figure 2.6** shows the competitive adsorption of water and ethanol on the active sites of the catalyst surface. Water is capable of irreversibly disassociating on the under-coordinated aluminium atoms on the catalyst surface to form stable surface hydroxyl species [17].

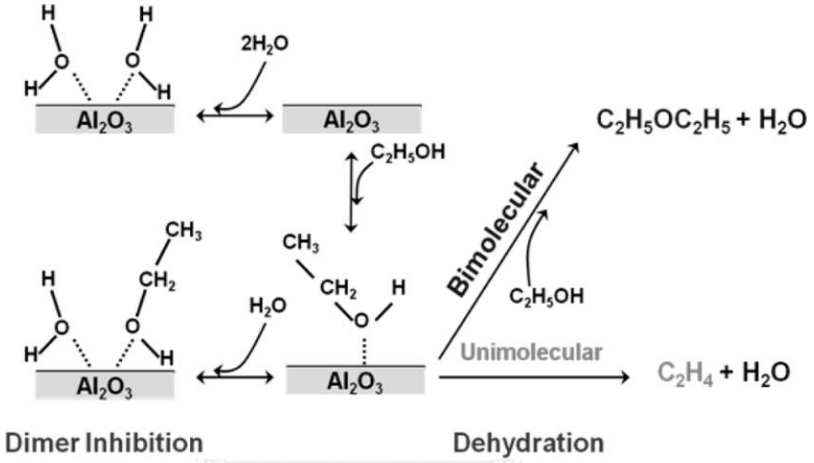

Figure 2.6 Mechanism of dimer formation from ethanol dehydration over γ-Al_2O_3 [17].

Moreover, Hydrolysis of Si-O-Al bonds is commonly reffered to as dealumination. Mechanisms for water-catalyzed dealumination as shown in **Figure 2.7**. During this reaction, aluminium atoms are removed from their framework positions, and silinol are formed. Dealumination starts with the breaking of the weakest Al–O bond rather than Si–O bond. When the weakest Al–O bond is broken, a water molecule coordinates to the tri-coordinated Al by forming an Al–OH group. The additional proton formed from hydrolysis of water attaches to the remaining Al–O–Si, but the rapid breaking of the remaining Al–O bonds results in its final state as part of the hydroxyl

group attached to Si in the form of Si–OH [18]. Therefore, Brønsted acid sites converted to Lewis acid sites.

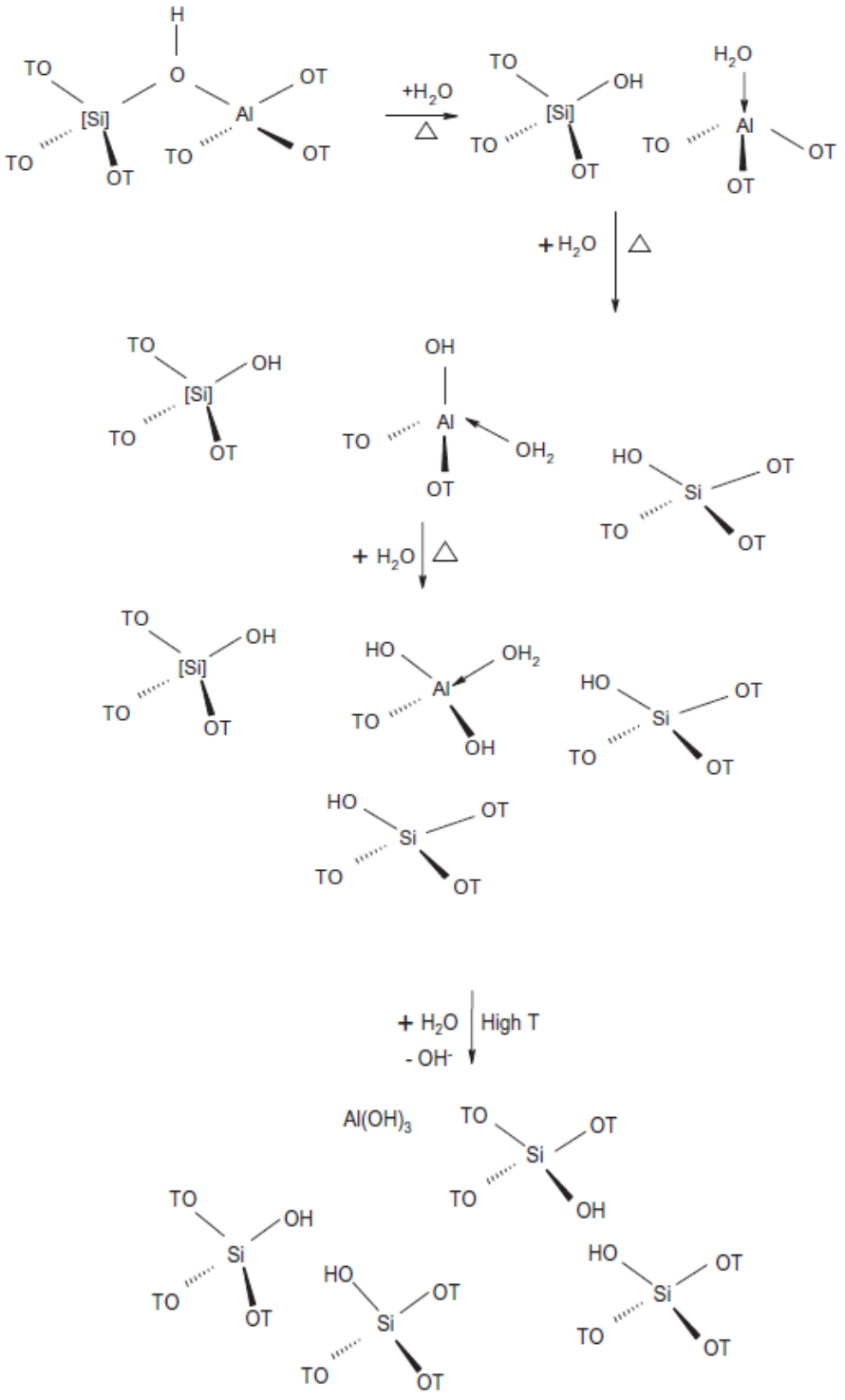

Figure 2.7 Mechanisms for water-catalyzed dealumination [18].

2.2 Alumina catalyst (Al_2O_3)

Alumina or aluminum oxide is a chemical compound of aluminium and oxygen with the chemical formula Al_2O_3. It is the most commonly occurring of several aluminum oxides, and specifically identified as aluminium (III) oxide. It is commonly called alumina, and may also be called aloxide, aloxite, or alundum depending on particular forms or applications.

The metastable Al_2O_3 structures, such as beta phase (γ-Al_2O_3), gamma phase (γ-Al_2O_3), alpha phase (α-Al_2O_3), theta phase (Θ-Al_2O_3), kappa phase (κ-Al_2O_3), chi phase (χ-Al_2O_3), eta phase (η-Al_2O_3) and delta phase (δ-Al_2O_3) [19].

The aluminum hydroxides exist in four well defined forms as shown below:

- The monohydrate AlOOH, as boehmite (γ-monohydrate) and diaspore (α-monohydrate)
- The trihydrate $Al(OH)_3$, as gibbsite (γ-trihydrate) and bayerite (α-trihydrate)

The transition phase of Al_2O_3 can be produced from heat treatment of aluminum hydroxides or aluminum salts as shown in **Figure 2.8.**

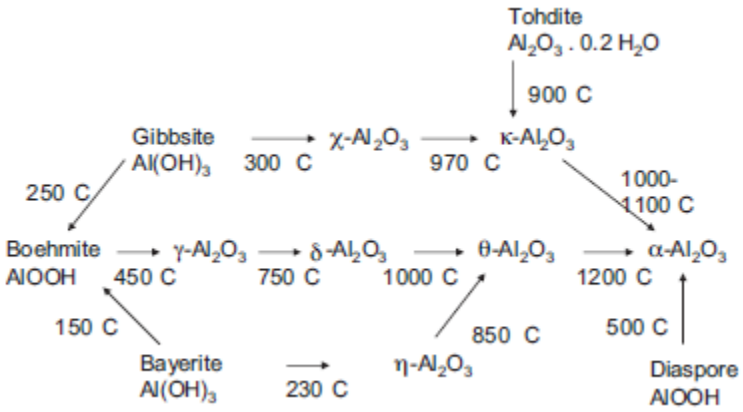

Figure 2.8 The structure transformation of alumina and aluminum hydroxides [20].

α- Al_2O_3 is the most stable form of the compounds formed between aluminum and oxygen, which is not porous as shown in **Figure 2.9**.

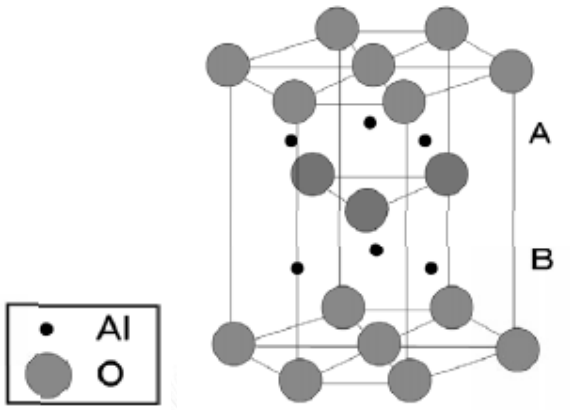

Figure 2.9 The structure of α-Al_2O_3 phase [19].

On the alumina surface, the acidity position is assigned by water molecules coordinated with Al^{3+} ions and cationic sites, whereas the basicity is assigned by O^{2-} anion vacancies and hydroxyl group [21].

2.3 Silica catalyst (SiO_2)

Silicon dioxide, also known as silica, is a chemical compound of oxide and silicon with the chemical formula SiO_2. Silica is most commonly found in nature as quartz, as well as in various living organisms. The operating temperature and pressure are the important factors affecting the structure formation of silica which can be either amorphous or crystalline.

Silica support can be utilized in many organic reactions with a large number of advantages such as a large surface area for solid state dispersion, thus they enhance the rate and yield of the chemical reactions [22].

Silica can synthesized in difference form, depending on Si-precursor and method. M41S is one of mesoporous silica, these materials have unique properties, such as a high specific surface area and pore volume, tunable pore size, and a narrow

pore size distribution. In this M41S family, three main phases have been described. The most well-known structure is the hexagonal MCM-41. The other two phases are the cubic MCM-48 and a lamellar phase, denoted as MCM-50 [9].

The composition of the synthesis gel has following molar ratio: 1TEOS: 0.3C16TMABr: $11NH_3$: xEthanol: $144H_2O$. Depending on the ethanol concentration in the TEOS-ammonia-water system, a succession of different mesophases in the order MCM-41 ⟶ MCM-48 ⟶ MCM-50 ⟶ SSP could be obtained at room temperature [23]. **Figure 2.10** illustrates that SSP has an excellent morphology due to the smoothness of spherical particles.

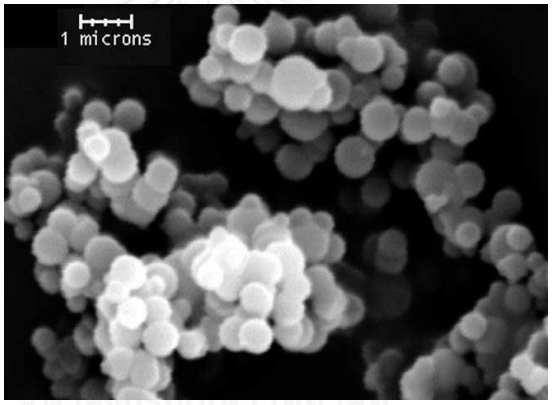

Figure 2.10 Morphology of SSP [23].

2.4 Alumina-silica catalyst

Alumina-silica are well-known solid acid catalysts, is used as a support or catalyst. The amorphous alumina-silica, typically prepared by co-precipitation or sol–gel methods and ion-exchanged. Solid acids catalyze a variety of transformations, including dehydration, isomerization, and cracking, and are used in processes such as fluid catalytic cracking (FCC) and methanol-to-gasoline (MTG) synthesis. The alumina-silica catalyst is a strong acid which has both has Lewis and Brønsted acid sites.

Silica and alumina are both very weak acids because of the high residual bonding strength of oxygen for hydrogen, while when Si^{4+} is isomorphically substituted by Al^{3+}, a negative charge is created in the structure, which is compensated by a proton. The proton is attached to the oxygen atoms, which is connected to the neighboring silicon and aluminum atoms and results in the so-called bridged hydroxyl group (Al–OH–Si). This site is responsible for the Brønsted acidity, while the three-coordinated Al atoms act as Lewis acid sites which can accept the lone pair of electrons [24]. Brønsted and Lewis acid site formation over the alumina-silica catalyst is shown in **Figure 2.11.**

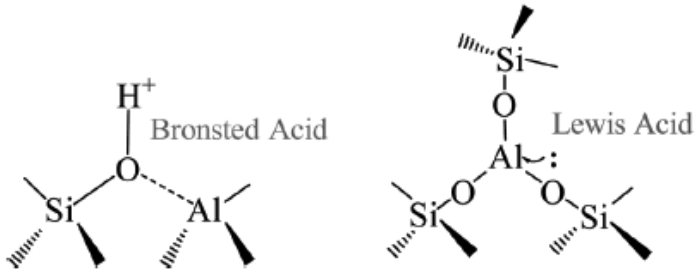

Figure 2.11 Brønsted and Lewis acid site formation over alumina-silica catalyst [24].

2.5 Sol-gel process

The sol-gel process is a wet chemical method for forming inorganic structures as powders, monoliths, fibers, or thin films from colloidal suspension of inorganic or metal organic precursors. The advantages of sol-gel processing include precise control of chemistry and structure at the molecular level, nano-sized porosity, and use of lower processing temperatures resulting in unique structures and lower associated costs [25].

A sol is a colloidal suspension of fine nano-sized particles in a liquid medium, typically an aqueous or alcohol solution with acid or base catalysts added to promote or control reactions. Typically, particles or polymer networks that form within the sol are 1-5 nm in size, but can be larger. Sols can also be formed from organic precursors

(usually metal alkoxides in alcohol or alcohol-water solutions). Hydrolysis of organic precursors is followed by condensation reactions resulting in polymer network formation and so-called polymeric sols. The polymer network structures can be weakly or highly branched with network interaction determining the sol structure. Sols can be formed from combined inorganic and organic precursors that, on reacting in solution, form a desired compound sol precursor. And then, the sol-gel process involves transformation of the sol to a gel. For sols formed from particulate precursors, particle agglomeration occurs with aging of the sol. Agglomerated particles of a certain size can remain separated in suspension as a result of repulsive forces due to surface charge effects overriding the reduction in surface free energy resulting from agglomeration. Particle agglomeration occurs when the attractive van der Waals force between particles is greater than the surface charge-related repulsive force. Increasing agglomerate size and, hence, reactant concentration result in an increased viscosity of the sol. This results in development of solution characteristics suitable for preparing components or coatings. Altering solution pH, which will affect the particle surface charge, will influence agglomeration. As agglomerate growth continues and viscosity increases, a continuous network eventually forms across a part dimension (either a bulk sample held in a mold, a film, or a thin coating). With this, the structure becomes self-supporting and transformation of a sol to a gel [25]. The steps in the sol-gel processing of materials and examples of the microstructures of final possible products are shown in **Figure 2.12**.

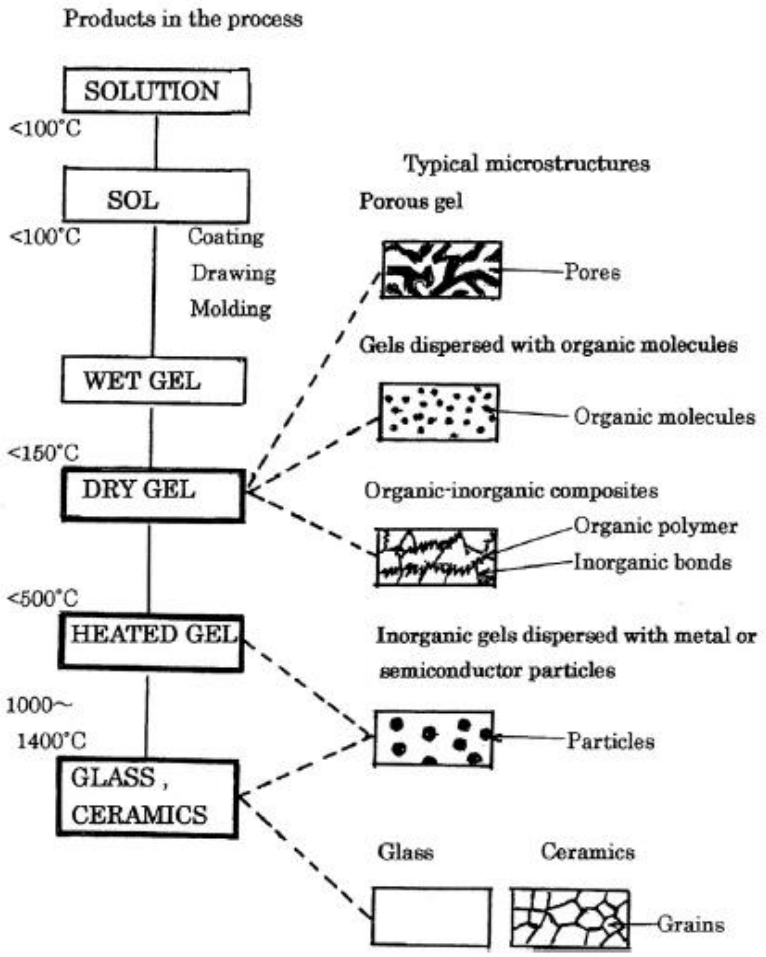

Figure 2.12 Steps of the sol-gel processing of materials and final products [26].

2.6 Catalyst deactivation

Catalyst deactivation is generally attributed to the deposition of carbonaceous species as well as either the sintering or oxidation of metallic particles.

Carbon may

1) chemisorb strongly as a monolayer or physically adsorb in multilayers and in either case block access of reactants to metal surface sites,

2) totally encapsulate a metal particle and thereby completely deactivate that particle, and

3) plug micro- and mesopores such that access of reactants is denied to crystallites inside these pores.

Finally, strong carbon filaments may build up in pores to the extent that they stress and fracture the support material, ultimately causing the disintegration of catalyst pellets and plugging of reactor voids [27]. Carbon (or coke) on the functioning of a supported metal catalyst are illustrated in **Figure 2.13**.

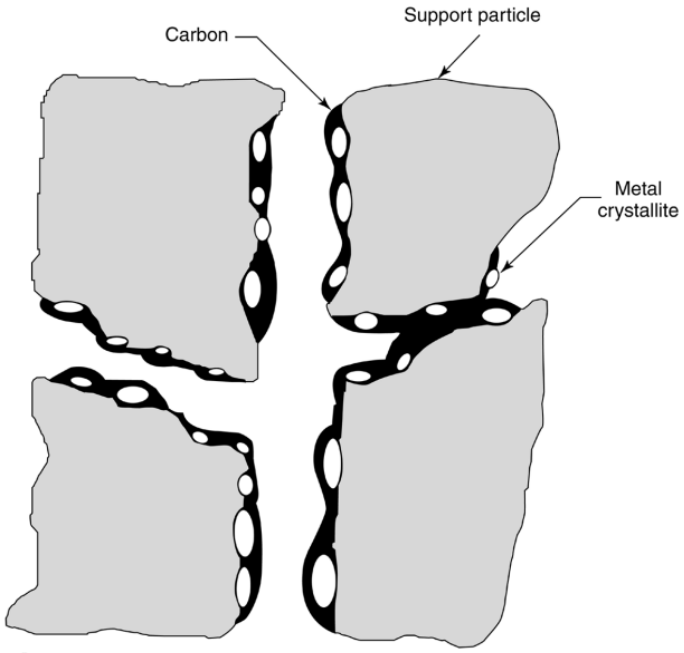

Figure 2.13 Coke formation on catalyst [27].

Some of the parallel reactions that take place with ethanol conversion reactions can also lead to catalyst deactivation. The main reactions that contribute to coke formation during ethanol conversion reactions are as follows [28]:

- Ethylene polymerization to coke:

  $C_2H_4 \longrightarrow$ coke (3)

- Acetone conversion to mesityl oxide:

  $2CH_3COCH_3 \longrightarrow (CH_3)_2C(OH)CH_2COCH \longrightarrow (CH_3)_2C{=}CHCOCH_3 + H_2O$ (4)

- Boudouard reaction:

$$2CO \longrightarrow CO_2 + C \quad (5)$$

- Reverse of carbon gasification:

$$CO + H_2 \longrightarrow H_2O + C \quad (6)$$

- Hydrocarbon decomposition:

$$CH_4 \longrightarrow C + 2H_2 \quad (7)$$

$$C_2H_4 \longrightarrow 2C + 2H_2 \quad (8)$$

The extent of each reaction depends on both reaction conditions and the catalyst used. While low reaction temperatures favor the formation of carbon through reactions 5 and 6, carbon formation via reactions 7 and 8 are the main routes at higher temperatures [28].

2.7 Literature reviews

2.7.1 Catalyst in Ethanol dehydration reaction

Zaki (2005) [29] studied catalytic dehydration of ethanol by using different prepared catalysts, which include Fe_2O_3, Mn_2O_3, and calcined physical mixtures of both ferric and manganese oxides with alumina and/or silica gel. The catalytic activities of such catalysts were tested through conversion of ethanol at 200–500 °C using a catalytic flow system operated under atmospheric pressure. However, the total ethanol conversion increased with increasing reaction temperature for all catalysts samples. The ethylene formation is increased with increased reaction temperature, while the diethyl ether formation is decreased. From the ethylene selectivity, it can be explained that the highest selectivity obtained by catalysts composed of iron–manganese oxides and of iron–manganese–silica oxides. Furthermore, the ethylene production selectivity depends on the catalyst chemical constituents. This result may

be concluded that the acid site on solid surface is important for ethanol dehydration to ethylene and diethyl ether.

Takahara *et al*. (2005) [30] investigated the dehydration of ethanol into ethylene over various solid acid catalysts, such as zeolites and silica–alumina, at temperatures ranging 453–573 K under atmospheric pressure. Ethylene was produced via diethyl ether during the dehydration process. The catalyst activity decreases in the following order: HM20>HM90>ZSM5-25>HB25>ZSM5-90>HY5.5>SA. H-mordenites were the most active for the dehydration. It was suggested that the catalyst activity could be correlated with the number of strong Brønsted acid sites in the catalyst. Furthermore, the H-mordenite was more stable with a SiO_2/Al_2O_3 ratio of 90 than with a SiO_2/Al_2O_3 ratio of 20.

Chen *et al*. (2007) [5] reported catalytic dehydration of ethanol to ethylene over TiO_2/γ-Al2O_3 catalysts. The conversion of ethanol and the selectivity of ethylene increase quickly with temperature rising, but the selectivity of diethyl ether is contrary. For γ-Al_2O_3, the conversion of ethanol is higher than 90% as the reaction temperature is higher than 460 ºC. The acid in TiO_2/Al_2O_3 can be regarded as moderate acid centers and the catalysts with moderate acid centers have relatively high activities for catalytic dehydration of alcohol. Therefore, the catalysts doped with 10 wt% TiO_2 have high ethanol conversions, ethylene selectivities and yields. The ethanol conversion of 99.96%, ethylene selectivity of 99.4% and ethylene yield of 26 g/(gcat·h) can be achieved. The selectivity of ethylene increases with decreasing ethanol concentration, while the selectivity of ethyl ether is on the contrary. This may be because L-acid shifts to B-acid more easily on γ-Al_2O_3 due to increased water concentration that leads to decreased alumina basicity and dehydration activities at the one hand.

Varisli *et al*. (2007) [31] investigated the dehydration reaction of ethanol in a temperature range of 140–250 °C with three different heteropolyacid catalysts, namely tungstophosphoricacid (TPA), silicotungsticacid (STA) and molybdophosphoricacid (MPA). Very high ethylene yields over 0.75 obtained at 250 °C with TPA was highly promising. At temperatures lower than 180 °C the main product was diethyl-ether. Presence of water vapor was shown to cause some decrease of catalyst activity. Results showing that product selectivities did not change much with the space time in the reactor indicated two parallel routes for the production of ethylene and DEE. Among the three HPA catalysts, the activity trend was obtained as STA>TPA>MPA.

Zhang *et al*. (2008) [4] studied the activity and stability of γ-Al_2O_3, HZSM-5 (Si/Al = 25), silicoaluminophosphate (SAPO-34) and Ni-substituted SAPO-34 (NiAPSO-34) as catalysts in the dehydration of ethanol to ethylene. SAPO-34 and NiAPSO-34 molecular sieves had been synthesized with hydrothermal method.γ-Al_2O_3 and HZSM-5 were commercial catalysts. NH_3–TPD study had revealed that substitution of Ni^{2+} for Al^{3+} in the SAPO-34 framework led to increase the weak and moderately strong acid strength and give rise to weak acid sites. Dehydration of ethanol was carried out over four catalysts and the results showed that ethanol conversion and ethylene selectivity decreased in the order HZSM-5 > NiAPSO-34 > SAPO-34 > γ-Al_2O_3. HZSM-5 sample possessing strong acidic property displayed the highest conversion of ethanol. As to the stability of catalyst, NiAPSO-34 and SAPO-34 were better than other two catalysts. NiAPSO-34 sample exhibited higher desorption temperature of both weak and strong acid sites and possessed more weak acid sites. Considering the activity and stability of the four catalysts comprehensively, NiAPSO-34 was the suitable catalyst in the dehydration of ethanol.

Xiao *et al*. (2009) [32] investigate the synergistic effect between the promoter and catalyst for ethanol dehydration to ethylene over TiO_2/4A zeolite composite catalysts that were prepared through coating TiO_2 on 4A zeolite via liquid phase deposition (LPD). The TiO_2/4A zeolite composite catalysts with higher surface weak acidity and lower mediate strong acidity exhibit much better catalytic performance on ethanol dehydration to ethylene compared with 4A zeolite. It is suggested that the TiO_2 promoter could improve the effective Lewis acidity of composite catalyst which consequently enhanced the catalytic performance. It is suggested that the catalytic performance of the catalysts is consistent with the effective Lewis acidity rather than the total acidity. As a result, with the increase of calcination temperature from 110 ºC to 600ºC, the effective Lewis acidity of the corresponding catalysts increases, so does the catalytic performance. The composite catalyst with mixed TiO_2 (A/R) has strongest effective Lewis acidity, hence shows the best catalytic performance.

Ramesh *et al*. (2009) [33] investigated the structural properties of nanocomposites of $LaPO_4$ and studied ethanol dehydration to over $LaPO_4$. $LaPO_4$ exhibited better catalytic activities compared to other metal phosphates, such as $ZrPO_4$ and $AlPO_4$, with the same P/metal ratio. Furthermore, the P/La ratio of $LaPO_4$ proved influential in the both ethanol conversion and ethylene selectivity. A P/La ratio of 2.0 exhibited very high activity during ethanol dehydration by selectively forming ethylene with a selectivity around 96% at 400 °C. Due to the increase in the medium strength acid sites, a high yield of ethylene was achieved. Hence, it can be concluded that the unique structure and the increase in surface area helps to provide more active sites, which improved the catalytic activity. Relatively low apparent activation energies between 18-38 kJ/mol were observed for these catalysts as compared to zeolites and other catalysts.

Chen *et al*. (2010) [34] studied the dehydration of ethanol to ethylene over modified silicoaluminophosphate (SAPO). SAPO-11 and SAPO-34 were commercial catalysts. Mn-SAPO-11, Zn-SAPO-11, Mn-SAPO-34 and Zn-SAPO-34 were synthesized with hydrothermal method. Mn^{2+} or Zn^{2+} modified SAPO-34 exhibited higher desorption temperature of both weak and strong acid sites and possessed more weak acid sites. Mn-SAPO-34 sample possessed the most amounts of weak acid sites while Zn-SAPO-34 possessed the most amounts of strong acid sites. According to catalytic mechanism of bio-ethanol dehydration, ethanol molecules chemically adsorbed on molecular sieve's active sites, generate firstly vinyl carbocation, then carbocation convert into ethylene. The increase of the weak acid sites and the acid amounts of both weak and strong acid sites, especially the amounts of weak acid sites, were helpful to catalytic activity for dehydration of ethanol to ethylene, while the too strong acidity will lead to ethylene polymerization. The conversion of ethanol and selectivity of ethylene decreased in the following order Mn-SAPO-34 > Zn-SAPO-34 > SAPO-11 > Mn-SAPO-11 > Zn-SAPO-11 > SAPO-34. The optimal reaction conditions were as the following: loading amount 5%, hydrothermal modification method, WHSV 2 h^{-1}, reaction time 10 h, reaction temperature 340 ºC, ethanol concentration 20%. The best yield of ethylene was up to 97.8% over Mn-SAPO-34 at the reaction temperature of 340 ºC at this optimal reaction conditions.

Zotov *et al*. (2011) [35] reported modification of Al_2O_3 with sulfate and chloride ions resulted in the increase in the catalytic activity in ethanol dehydration. The concentrations of the weak and strong acceptor sites increased as well. Meanwhile, the concentration of the electron donor sites decreased. This observation suggests that the donor sites are not related to the active sites in the ethanol dehydration. However, a remarkably good correlation between the concentration of the weak donor sites and the catalytic activity of the acid modified catalysts almost passing through

the origin of coordinates was obtained for all the studied samples. So, it appears that the weak acceptor sites tested using anthracene are related to the sites active in the ethanol dehydration reaction. Most likely, both reactions are initiated by sufficiently strong Brønsted acid sites. A similar correlation may be expected for this reaction over other heterogeneous acid catalysts, including supports other than alumina.

Wang *et al*. (2011) [36] studied coking behavior of a submicron MFI zeolite catalyst for ethanol to ethylene in a pilot scale tubular reactor. The submicron MFI catalysts possessed high activity and stability. Ethanol conversion and ethylene selectivity over the fresh/regenerated catalyst were around 97.9%/96.2% and 99.1%/98.9%, respectively. The fresh catalyst illustrated an active duration of 1606 h, while the regenerated of 2008 h, which implied the regeneration can enhance the stability. In the reactor, the coke mainly consisted of adsorbed substances at the forepart and of alkyl aromatics at the end, and the coke contents presented an approximate U-shape trend along the tube length. Further tests revealed that the loss of acidity rather than the pore volume should be responsible for the catalyst deactivation.

León *et al*. (2011) [37] investigated the ethanol catalytic condensation over different Mg–Al mixed oxides derived from hydrotalcites. The studied catalysts are active for both dehydration reaction yielding ethylene (because of the presence of acid sites) and hydrogenation reactions yielding acetaldehyde (catalyzed by medium-strength basic sites). Acetaldehyde is the key reactant for condensation reaction, yielding 2-butenal as primary condensation product. This reaction is catalyzed by the strongest basic sites. This unsaturated aldehyde undergoes successive hydrogen transfer reactions and/or dehydrations yielding different C4 chemicals: 2-buten-1-ol, butanal, 1-butanol, 1,3-butadiene and 1-butene. Although the total conversion

obtained with the different materials is rather similar, important differences are observed in the obtained selectivity. Those materials with higher concentration and strength of the basic sites are those more selective for C4 fractions, whereas the presence of acid sites promotes ethanol dehydration, decreasing the efficiency for condensation reactions.

Bedia *et al*. (2011) [38] studied gas phase ethanol decomposition over acid carbon catalysts .The acid carbon catalysts were obtained by chemical activation of olive stone with phosphoric acid, without needing additional oxidative treatments. The amount of stable phosphorus remaining over the carbon surface after the washing process increases with both activation temperature and impregnation ratio. The increase of the activation temperature results in an increase in the proportion of C_3PO and C_3P surface groups. In carbon catalysts, surface acidity, predominantly of Brønsted type, was dependent on the amount of phosphorus retained on the carbon surfaces. Catalysts HA1-800 shows initial conversion higher than 90% at 350 °C. For all the carbons, the main product is ethylene, although at low conversion the selectivity to diethyl ether is higher than that to ethylene. The catalytic decomposition of ethanol over the activated carbons yields mainly dehydration products, mostly ethylene with lower amounts of diethyl ether.

Bokade and Yadav (2011) [39] studied the dehydration of dilute bio-ethanol (80%m/m) over three different heteropolyacid catalysts namely, dodecatungestophosphoric acid (DTPA), phosphomolybedic acid (PMA) and sodium tungstate hydrated purified (STH) supported on montmorillonite. The 30%m/m DTPA/montmorillonite was more acidic than other studied catalysts. 30% m/m DTPA/montmorillonite showed the maximum number of acid sites (28.2%) as compared to 30%m/m PMA/montmorillonite (20.9%) and 30%m/m

STH/montmorillonite (10.3%). The loading of different heteropolyacids on plain clay catalyst led to an increase in the concentration of acid sites by 10.3%, 20.9% and 28.2% respectively. 30%m/m DTPA/K-10 was found to be more active with 74% ethanol conversion and 92% ethylene selectivity at 250 °C in comparison with other acid catalysts used.

Han *et al*. (2011) [40] investigated the effect of calcination temperature on the catalytic performance of the dehydration of aqueous ethanol on Mo/HZSM-5 prepared by impregnation. 5 wt% Mo/HZSM-5 catalyst calcined at 500 °C exhibited the highest weak and medium acidity and much better catalytic performance in ethanol dehydration reaction compared with HZSM-5. The Mo species on the external surface of HZSM-5 was easier to be reduced during the reaction. Combining quantitative analyses of NH_3-TPD and H_2-TPR profiles of fresh and used catalysts revealed that the decrease of weak and medium acidity could be correlated with the reduction of Mo species. It is proposed that reduction of Mo species caused the decrease of weak and medium acidity, which contributed to activity drop at the initial reaction stage.

Matachowski *et al*. (2012) [41] investigated the gas-phase dehydration of ethanol over neutral silver salt of tungstophosphoric acid $Ag_3PW_{12}O_{40}{\cdot}3H_2O$ (AgPW) in the temperature range of 373–493 K. The relative humidity of atmosphere (nitrogen or air) was changed from 2% to 10%. It was shown that relative humidity of both atmospheres strongly influences the catalytic activity of AgPW salt. The AgPW salt is stable, when relative humidity attains at least 10% independent of atmosphere in which reaction is performed. In such conditions and at 473 K the AgPW catalyst exhibited the conversion of ethanol as well as the selectivity to ethylene about 99%. It can be concluded that $Ag_3PW_{12}O_{40}{\cdot}3H_2O$ salt can be used as an ‘ecofriendly’ catalyst

for ethylene production by the dehydration of ethanol in nitrogen or air atmospheres in relatively low temperature and appropriate relative humidity.

Phung *et al*. (2014) [16] investigated the conversion of ethanol over four commercial aluminas prepared by different industrial procedures and one commercial silica-alumina. Total conversion of ethanol with >99% selectivity to ethylene is achieved at 623 K over the purer Al_2O_3 catalyst (Na < 0.002 wt%). The most active sites are believed to be Lewis acidic Al^{3+} sites in a tetrahedral environment located on edges and corners of the nanocrystals. Ethanol adsorbs dissociatively on Lewis acid-base pair sites but may also displace water and/or hydroxyl groups from Lewis acidic Al^{3+} sites forming the active intermediate ethoxy species. Surface ethoxy groups are supposed to be intermediate species for both diethyl ether and ethylene production. Silica-alumina also works as a Lewis acid catalyst. The slightly lower activity on surface area basis of silica-alumina than aluminas attributed to the lower density of Lewis acid sites and the absence of significant basicity.

Mahmoud (2014) [42] reported Cr_2O_3–ZrO_2 binary oxide catalysts (CZ) with molar Zr/(Zr + Cr) ratio equals 75% (CZ75), in particular, exhibited significantly higher specific surface areas and porosity than other composites and pure oxides. The catalytic conversion of ethanol was studied at 200–400°C. The catalytic activities exhibited by the binary oxides were significantly higher than those of the pure oxides. The CZ75 nanomaterial being the most active while the CZ0 being the less active one. The most active catalyst, CZ75, is the one in which high surface area of binary oxide enables very strong dispersion of ZrO_2 on Cr_2O_3 surface providing a higher number of active phases to participate in ethanol conversion. The total ethanol conversion (TC%) and dehydration/dehydrogenation selectivity were dependent on the Cr/Zr ratio.

Phung *et al*. (2015) [43] investigated the ethanol dehydration at atmospheric pressure with 1.43 h^{-1} WHSV in nitrogen, in the temperature range 423–773 K over titania and zirconia, as such and modified by addition of WO_3. The results shown that $WO_3/ZrO_2$and WO_3/TiO_2 are excellent catalysts for ethanol dehydration. The addition of WO_3 to both ZrO_2 and TiO_2 introduces strong Brønsted acid sites that are supposed to represent the active sites in the reaction, but also inhibits the formation of byproducts, such as acetaldehyde. This is attributed to the poisoning of basic sites and of reducible surface Ti and Zr centres, respectively.

Phung *et al*. (2015) [3] investigated the ethanol dehydration over commercial H-FER, H-MFI, H-MOR, H-BEA, H-Y and H-USY zeolite samples, and alumina and silica-alumina for comparison. H-zeolites are definitely more active than silica-alumina and alumina on catalyst weight base. The H-MOR sample is the most active but the H-MFI samples with Si/Al ratios 280 and 50 show higher reaction rates per Al ion, H-FER and faujasites show highest ethylene yield (99.9% at 573 K). At lower temperature and higher space velocities, diethyl ether is formed with high yield (>70% at 453–473 K on H-BEA and H-MFI (50)). Over conversion of ethylene mainly to aromatics is observed on H-MFI (50). The different behavior of protonic zeolites can predominantly be explained by confinement effects on the different zeolite cavities. Among zeolite samples, an activity (per catalyst weight) trend H-MOR, 16.3% > H-MFI (50), 11.5% > H-BEA, 7.7% ≈ H-FER, 7.0% > H-MFI (280), 4.6% ≈ H-USY, 2.5% > H-Y, 1.2% is found, e.g. 413 K.

2.7.2 The ethanol dehydration over silica-alumina catalyst

Phung and Busca (2015) [14] studied the catalytic conversion of ethanol and diethyl ether (DEE) over alumina, zeolites MFI, FER and USY, silica–alumina and calcined hydrotalcite. Zeolites, alumina and silica–alumina are active in the temperature range 453–573 K for both ethanol dehydration to DEE and to ethylene and for DEE cracking and hydrolysis, producing back ethanol and ethylene. Protonic zeolites are more active than alumina which is slightly more active than silica–alumina for these reactions. Ethanol dehydration to DEE occurs selectively at lower temperature with a ‘‘bimolecular’’ mechanism involving reaction of ethoxy groups with undissociated ethanol. Ethanol dehydration to ethylene occurs selectively at relatively high temperature with an elimination mechanism via decomposition of ethoxy groups over these catalysts, but also occurs, at lower temperature, with a consecutive path via DEE formation and cracking.

Phung and Busca (2015) [15] investigated the catalytic activity of catalysts in ethanol dehydration. The trend of ethanol conversion in the experiments performed using the same catalyst weight is γ-Al_2O_3 (A) > SA87 > SA30 > SA5 >> SiO_2 (S). The catalytic activity of silica-alumina seems to slightly decrease in parallel with increasing SiO_2/Al_2O_3 ratio. In all cases the materials present strong Lewis acidity together with Brønsted sites able to protonate pyridine. These materials show high activity in ethanol conversion to ethylene and diethyl ether. The diethyl ether/ethylene selectivity depends on the nature of the active site, diethyl ether formation being more favored for lower SiO_2/Al_2O_3 ratios where Lewis sites are more frequently surrounded by alumina-like surface.

CHAPTER III

EXPERIMENTAL

3.1 Catalyst preparation

3.1.1 Chemicals

- Tetraethyl orthosilicate ($Si(OC_2H_5)_4$, Aldrich 98%)
- Cetyltrimethylammonium bromide ($CH_3(CH_2)_{15}N(Br)(CH_3)$, Aldrich 98%)
- De-ionized water
- Ethanol (VWR chemicals 99.98%)
- Ammonia (Panreac 30%)
- Ammonium nitrate nonahydrate ($Al(NO_3)_3 \cdot 9H_2O$, Aldrich 98%)

3.1.2 Synthesis of the spherical silica particle and alumina-silica composite catalyst

The first, xAl-SSP was prepared with the following molar ratio: 1TEOS: 0.3CTAB: $11NH_3$: 58Ethanol: $144H_2O$ [23]. This solution was stirred at room temperature for 1 hour. Secondly, adding ammonium nitrate into the solution and stirred at room temperature for 1 hour. After that, the white precipitate was separated from solvent by centrifuge. Then, the sample was dried at 110 ºC for 24 hours. Dried sample was calcined in air at 700 ºC for 6 hours. The nomenclature of catalyst is xAl-SSP (where x = 20, 40, 50, 60 and 80 mol%).

3.2 Catalyst characterization

3.2.1 X-ray diffraction (XRD)

X-ray diffraction (XRD) patterns of SSP, 40Al-SSP and 80Al-SSP catalysts were measured by the SIEMENS D5000 X-ray diffractometer. The experiment was carried out by using Cu K_α radiation source with Ni filter in the 2θ range of 10-80 degrees with a resolution of 0.02°.

3.2.2 Scanning electron microscopy (SEM) and energy x-ray spectroscopy (EDX)

The morphology and elemental dispersion over the catalysts surface were determined by scanning electron microscope (SEM) and energy X-ray spectroscopy (EDX), respectively. The SEM model is JEOL mode JSM-5800LV and Link Isis Series 300 program was performed for EDX.

3.2.3 Nitrogen physisorption (BET)

The surface area, pore volume and pore diameter of all catalysts were determined by nitrogen gas adsorption at liquid nitrogen temperature (-196 °C) using micromeritics chemisorb 2750 pulse chemisorption system instrument.

3.2.4 Temperature programed adsorption (NH_3-TPD)

The acid properties of catalysts were investigated by temperature programmed desorption of ammonia (NH_3-TPD) equipment by using micromeritics chemisorb 2750 Pulse chemisorption system. In an experiment, a quarts wool 0.03 g and 0.1 g of catalyst was loaded in a glass tube and pretreated at 400 °C with helium flow for an hour. The sample was saturated with 15%NH_3/He at 120 °C for an hour. After that, the physisorbed ammonia was desorbed in a helium gas flow. Then, the sample was

heated from 35-750 ºC with a heating rate of 10 ºC/min. The amount of desorbed ammonia was measured via TCD signal as a function of temperature.

3.2.5 Fourier transform infrared spectroscopy (FTIR)

FT-IR analysis was used to determine the functional group as the chemical structure of alumina-silica using a Nicolet 6700 FTIR spectrometer. Infrared spectra were recorded with FTIR spectrometer and range of scanning from 400 to 4,000 cm^{-1}.

3.2.6 Thermal gravimetric analysis (TGA)

Thermal gravimetric analysis (TGA) was used to study the thermal decomposition of alumina-silica catalyst under the temperature range of room temperature to 1000 ºC with a heating rate of 10 ºC /min in nitrogen atmosphere using an STD analyzer model Q600 from TA instrument.

3.2.7 X-Ray Fluorescence (XRF)

The element and chemical analysis was determined by X-ray fluorescence spectrometer using Pana analytical MINIPAL4 analyzer. The 1 g of catalyst was used.

3.3 Ethanol catalytic dehydration test

In this research, the catalytic activity of all catalyst was investigated by using the experimental set-up apparatus as show in **Figure 3.1**

3.3.1 Chemicals and reactants

- High purity grade hydrogen gas (99.999%) (TIG)
- Ultra high purity nitrogen gas (99.999%) (TIG)
- Ultra high purity argon gas (99.999%) (TIG)
- Absolute ethanol (99.98%) (VWR CHEMICALS)

3.3.2 Instruments and apparatus

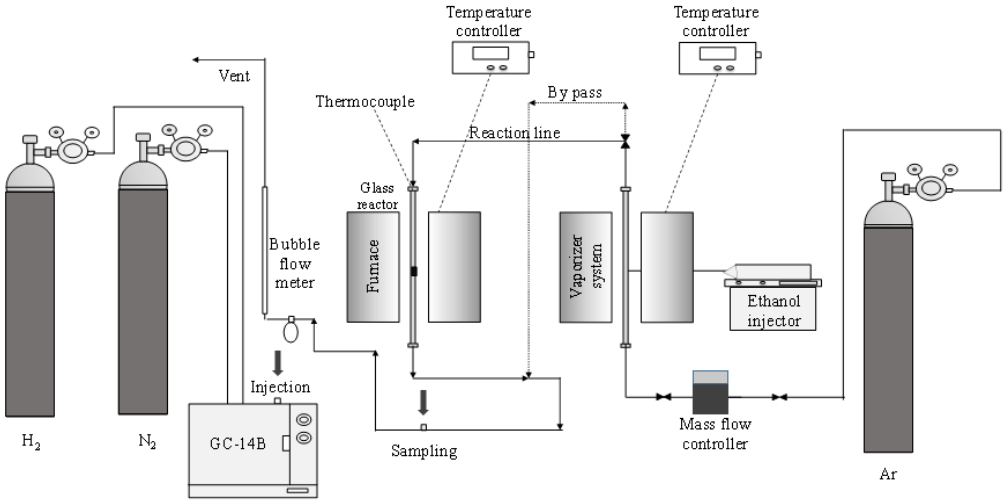

Figure 3.1 Experimental set-up for reaction test.

From **Figure 3.1**, the Experimental set-up for reaction tests consists of:

a) *Reactor*: The reactor is made from glass tube which is borosilicate type with an inside diameter of 0.7 mm.

b) *Vaporizer*: The vaporizer is equipment to vaporize ethanol from liquid phase to vapor phase. It is operated at temperature of 120 °C at

atmospheric pressure. This temperature is higher than the boiling point of ethanol (78.37 ºC), thus ethanol can be vaporized.

c) *Syringe pump*: The syringe pump is used to inject ethanol into vaporizer at fixed rate of 1.45 ml/h.

d) *Furnace and heating tape*: The furnace is heated to the catalyst fixed-bed reactor tube. The temperature of the furnace is controlled by temperature controller. For heating tape, it is covered on outlet of the pipeline to prevent the condensation of product.

e) *Temperature controller* :

- At furnace, the temperature of furnace is set at temperatures in range between 200°C to 400°C.

- At vaporizer, the temperature is set at 120 ºC. (Above the boiling point of product from ethanol dehydration)

f) *Gas system*: Argon is a carrier gas, which is used to carry ethanol vapor into the furnace and reactor. The flow rate of carrier gas is controlled by mass flow controller.

g) *Sampling*: The sample is collected at sampling with 1.0 ml of product to analyze by GC.

h) *Gas chromatography (GC)*: A Gas chromatography is used for investigating ethanol conversion and product selectivity. It equipped (Shimadzu GC-14B) with flame ionization detector (FID) with DB-5 capillary column.

The operating condition for gas chromatography is reported;

- Detector: FID
- Capillary column: DB-5
- Carrier gas: Nitrogen (99.99 vol. %) and Hydrogen (99.99 vol. %)
- Column temperature

- Initial: 40 °C
- Final: 40 °C

- Injector temperature: 150 °C
- Detector temperature: 150 °C
- Time analysis: 7 min
- Analyzed gas: ethanol, ethylene, diethyl ether, acetaldehyde

3.3.3 Ethanol dehydration reaction procedure

The ethanol dehydration was carried out in a fixed bed down flow reactor with an inner diameter 0.7 mm at atmospheric pressure. In the experiment, 0.01 g of a packed quartz wool and about 0.05 g of catalyst was loaded into the reactor. First, a carrier gas (argon) at flow of 60 ml/h was fed into the reactor to pre-heat the catalyst at 200 °C for 1 h. A syringe pump was used to inject ethanol into the vaporizer at a fixed rate (1.45 ml/h). Ethanol was saturated in vaporizer system at 120 °C and it was fed into the reactor. The reaction temperature increased from 200 °C to 250 °C, 300 °C, 350 °C, and 400 °C in each run. Finally, The product of 1.0 ml (gas phase) in each temperature was injected into the Shimadzu GC8A gas chromatograph with FID using capillary column (DB-5) at 150 °C. The conversion data in each temperature is an average value.

CHAPTER IV
RESULTS AND DICUSSION

In this chapter describes the characterization and catalytic activity of spherical silica particle and alumina-silica composite catalysts in dehydration reaction of ethanol. The characteristic of all catalyst was investigated by thermal gravimetric analysis (TGA), X-ray diffraction (XRD), Fourier transform infrared spectroscopy (FTIR), scanning electron microscopy (SEM), energy dispersive X-ray spectroscopy (EDX), X-ray fluorescence spectrometry (XRF), temperature programmed desorption of ammonia (NH_3-TPD) and nitrogen physisorption. This chapter is divided into three parts. In the first part, the activity and selectivity of Al-SSP composite catalysts for the dehydration reaction of ethanol were determined. In the second part, the effect of ethanol concentration of Al-SSP composite catalysts for the dehydration reaction of ethanol was studied. Finally, the stability of Al-SSP composite catalysts for the dehydration reaction of ethanol was illustrated in the last part.

4.1 Characterization and catalytic activity of spherical silica particle (SSP) and alumina-silica composite catalysts (Al-SSP).

4.1.1 X-ray fluorescence (XRF)

The composition and amount of element in catalyst bulk were analyzed by X-ray fluorescence as shown in **Table 4.1**. The SiO_2/Al_2O_3 molar ratio decreased with increasing Al content except 80Al-SSP catalysts. Moreover, the maximum amount of Al_2O_3 of all alumina silica catalyst is ~ 38 mol%.

Table 4.1 The amount of element distribution of SSP and all composite catalysts obtained from XRF.

Catalysts	Amount of mole in catalyst (mol%)		SiO_2/Al_2O_3 molar ratio
	Al_2O_3	SiO_2	
SSP	-	100	-
20Al-SSP	7.87	92.13	11.71
40Al-SSP	24.05	75.95	3.16
50Al-SSP	31.08	68.92	2.22
60Al-SSP	37.96	62.04	1.63
80Al-SSP	26.14	73.86	2.83

4.1.2 X-ray diffraction (XRD)

XRD is used for identification of the crystal phase and crystallite size of each phase present. XRD patterns of Al-SSP composite catalysts calcined at 700 ºC are shown in **Figure 4.1.** For All Al-SSP composite catalysts, the broad peaks from 20º to 30º attributed to amorphous silica-alumina were also observed. At lower Al content, such as 20Al-SSP, 40Al-SSP and 50Al-SSP, there are no diffraction peaks of the crystalline γ-alumina phase (46º and 67º) in the XRD pattern, suggesting that γ-alumina in this sample exists in a highly dispersed state on silica surface. At higher Al content, i.e. 60Al-SSP, the characteristic peaks of γ-alumina were visible. However, the characteristic peaks of the crystalized γ-alumina phase were not observed in 80Al-SSP.

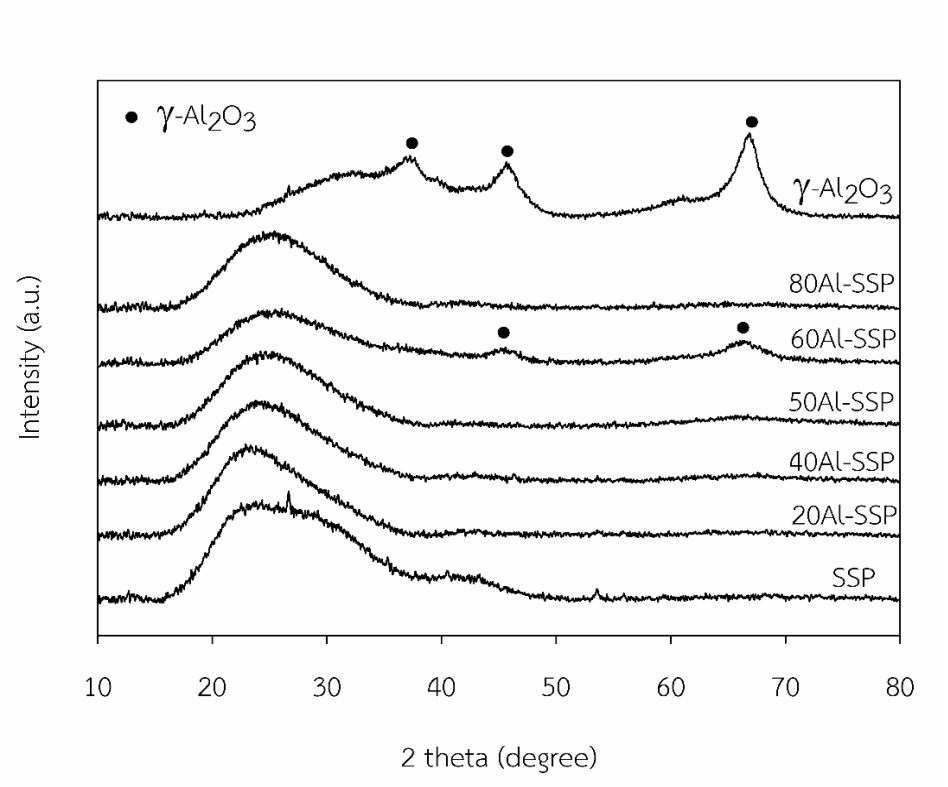

Figure 4.1 XRD patterns of γ-alumina, spherical silica particle and all alumina-silica composite catalyst calcined at 700 ºC.

4.1.3 Thermal gravimetric analysis (TGA)

In order to decide on the calcination temperature of the prepared catalyst, TGA analysis was carried out. As illustrated in the TGA curve given in **Figure 4.2**, three stages weight loss of the synthesized material was observed at 200 ºC and 240 ºC. A small peak was also observed at about 500 ºC. The catalyst precursor appeared to have undergone three stages of decomposition reactions with a total weight loss of ~50%. The first step corresponds to an endothermic weight loss of ~18%, which is attributable to the removal of adsorbed water and nitrate decomposition (in all Al-SSP composite catalyst) below 200 ºC. The second broad exothermic weight loss observed in the temperature range of 215-240 ºC is essentially due to the removal of the surfactant (CTAB) from the synthesized material, followed by a third process above 500 ºC, which

is attributable to a loss due to the slow continuous dehydroxylation [44]. The broad exothermic peak ranging from 400 ºC to 800 ºC may be ascribed to the crystallization of γ-alumina or other forms of alumina [44].

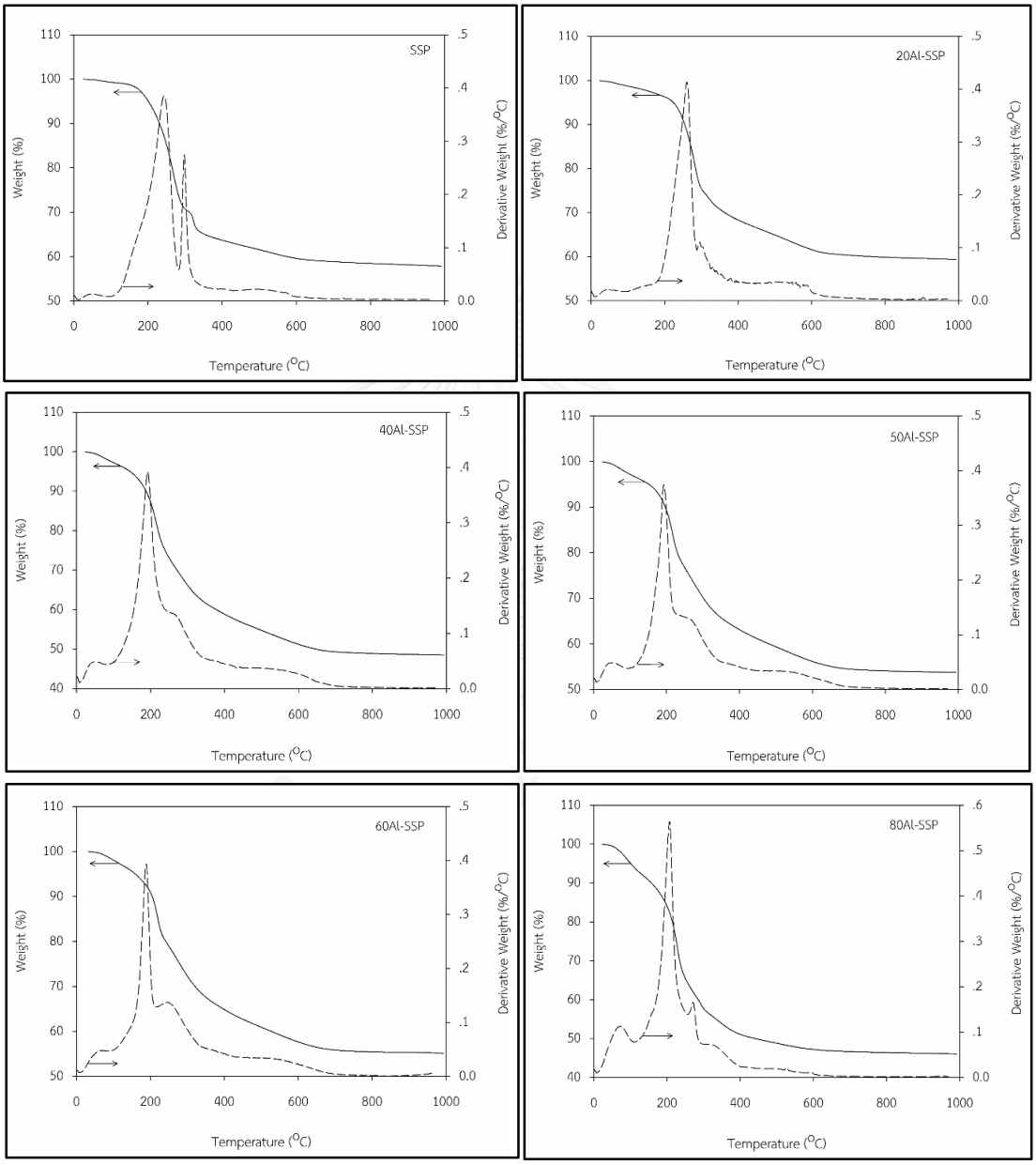

Figure 4.2 DTA/TGA curves of spherical silica particle and all alumina-silica composite catalyst calcined at 700 ºC.

4.1.4 Fourier transform infrared spectroscopy (FTIR)

The FTIR spectra of SSP and all alumina-silica composite catalyst calcined at 700 °C are provided in **Figure 4.3** and **Figure 4.4**. For SSP and Al-SSP composite catalysts, the peaks at 3420 cm^{-1} and 1645 cm^{-1} are respectively assigned to the stretching and blending modes of hydroxyl groups, which are attached to the surface of all catalysts (mainly Si-OH groups) and adsorbed water molecule. The peak at 1059 cm^{-1} is characteristic of Si-O stretching vibration of Si-O-Si while the peak at 815 cm^{-1} are ascribed to Si-O stretching vibration of Si-O-Al [45] that was not observed in SSP catalyst. This refers that the chemical bonding between alumina and silica was occurred after the calcination at 700 °C. Another band was observed at about 472 cm^{-1} indicating the presence of O-Si-O bending vibration. Moreover, the peak of OH vibration at about 3420 cm^{-1} increased when alumina content in SSP increased.

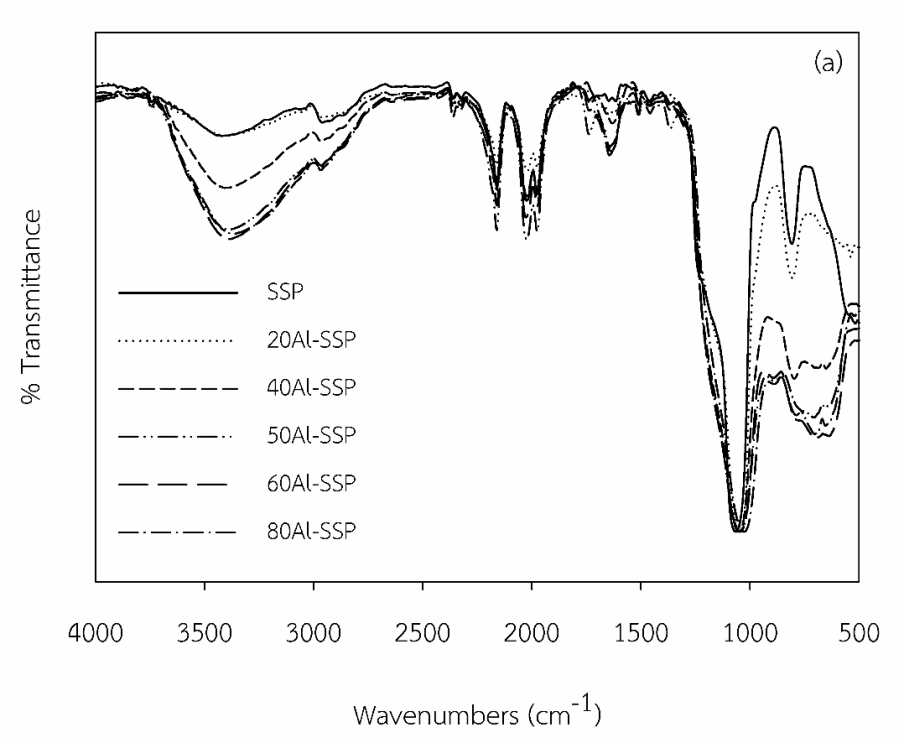

Figure 4.3 FTIR spectra of spherical silica particle and all alumina-silica composite catalyst calcined at 700 °C.

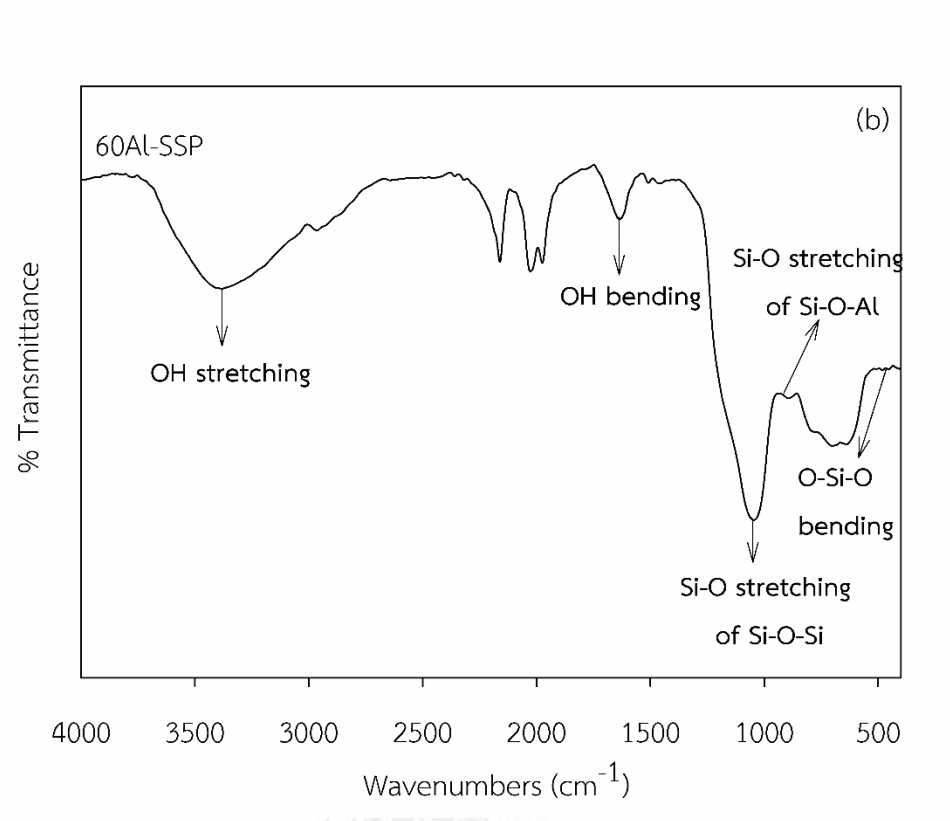

Figure 4.4 FTIR spectra of 60Al-SSP catalyst calcined at 700 °C.

4.1.5 Scanning electron microscopy (SEM)

The morphology of SSP and all alumina-silica composite catalyst was investigated by SEM technique, which are illustrated in **Figure 4.5**. It was found that the morphology of SSP was spherical with average size of ~0.6 μm. When adding alumina into silica particle, the morphology of alumina-silica composite catalyst are identified in large aggregates. Moreover, the alumina particle covered on silica surface as shown in the image of all alumina-silica composite catalyst.

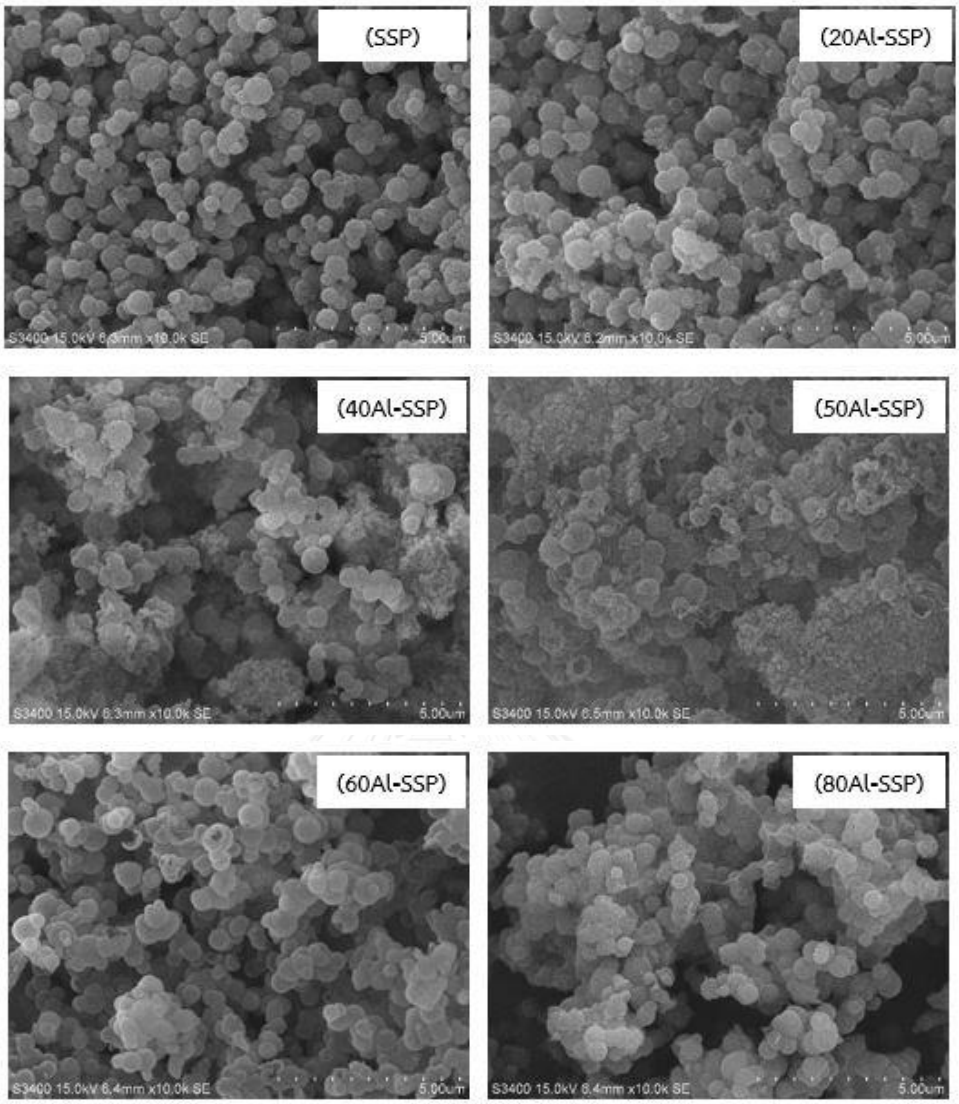

Figure 4.5 SEM images of spherical silica particle and all alumina-silica composite catalyst.

4.1.6 Energy dispersive X-ray spectroscopy (EDX)

The amount of element distribution on surface of SSP and all composite catalysts was characterized by EDX technique as shown in **Table 4.2**. The amount of alumina on the surface of all alumina silica composite catalysts also increased with increasing Al content. The amount of oxygen on the surface of all catalysts were not significantly different. In part of silica, the amount of silica slightly decreased due to replacement with alumina particle during catalyst preparation. Moreover, the Al/(Al+Si)

molar ratio increased with increasing Al content, but in the 60Al-SSP and 80Al-SSP, It was not significantly different. The trend of Al/(Al+Si) molar ratio is 80Al-SSP ≈ 60Al-SSP > 50Al-SSP > 40Al-SSP > 20Al-SSP >> SSP. This result indicated that the 60Al-SSP solution containing the maximum concentration of aluminium nitrate dissolved in the solvent mixture. Furthermore, the different Al/(Al+Si) molar ratio affects to the amount of acid sites for catalysts.

Table 4.2 The amount of element distribution on surface of SSP and all composite catalysts obtained from EDX.

Catalysts	Amount of mole on surface (mol%)			
	Al	Si	O	Al/(Si+Al)
SSP	0.00	34.57	65.43	0.00
20Al-SSP	2.99	34.42	62.59	8.00
40Al-SSP	5.60	32.97	61.43	14.52
50Al-SSP	14.35	26.03	59.62	35.55
60Al-SSP	14.63	22.23	63.14	39.69
80Al-SSP	15.58	23.71	60.71	39.65

The elemental distribution on surface of all catalysts was detected by energy dispersive X-ray spectroscopy (EDX) method. The EDX mapping of all catalysts are shown in **Figure 4.6** to **Figure 4.11**. The element compositions on outer surface of Al-SSP composite catalyst include Al, Si and O. It suggested that alumina covered on the surface of the spherical silica particle is well dispersed.

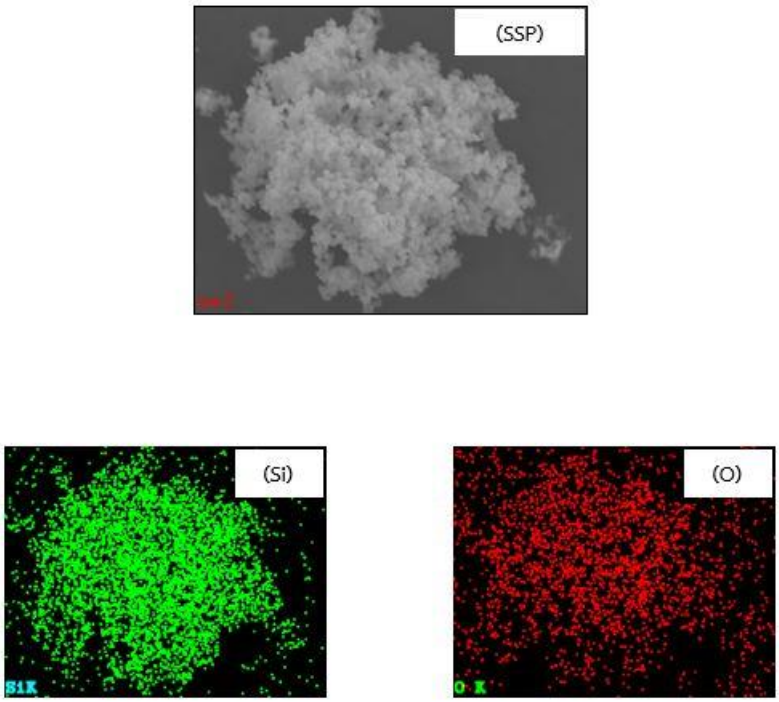

Figure 4.6 EDX mapping of spherical silica particle.

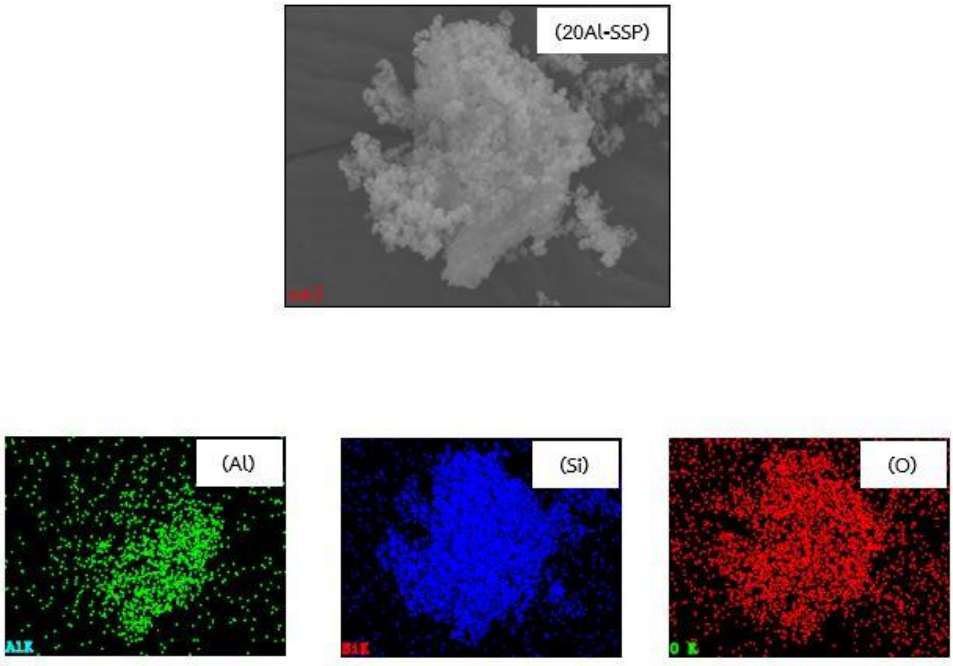

Figure 4.7 EDX mapping of 20Al-SSP catalyst.

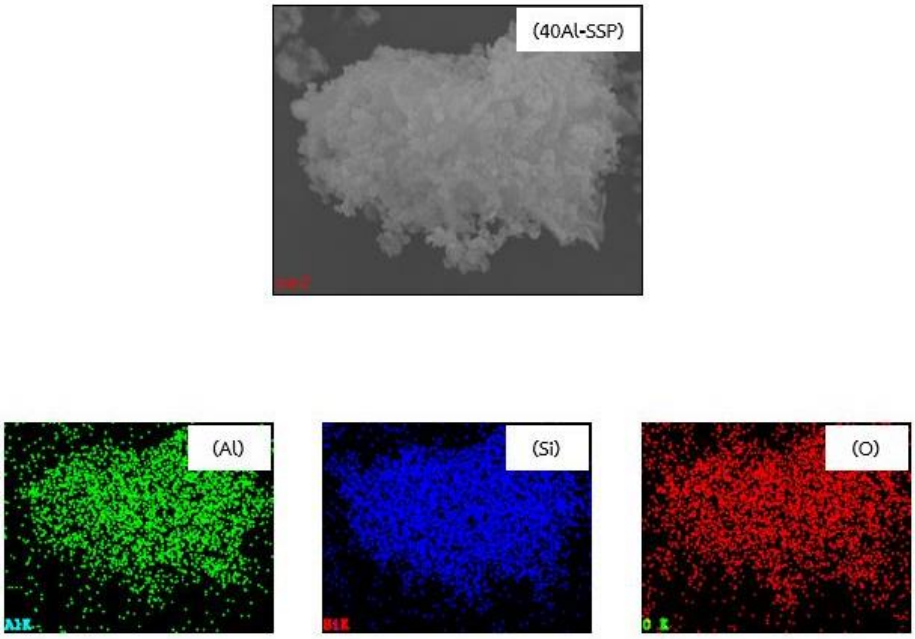

Figure 4.8 EDX mapping of 40Al-SSP catalyst.

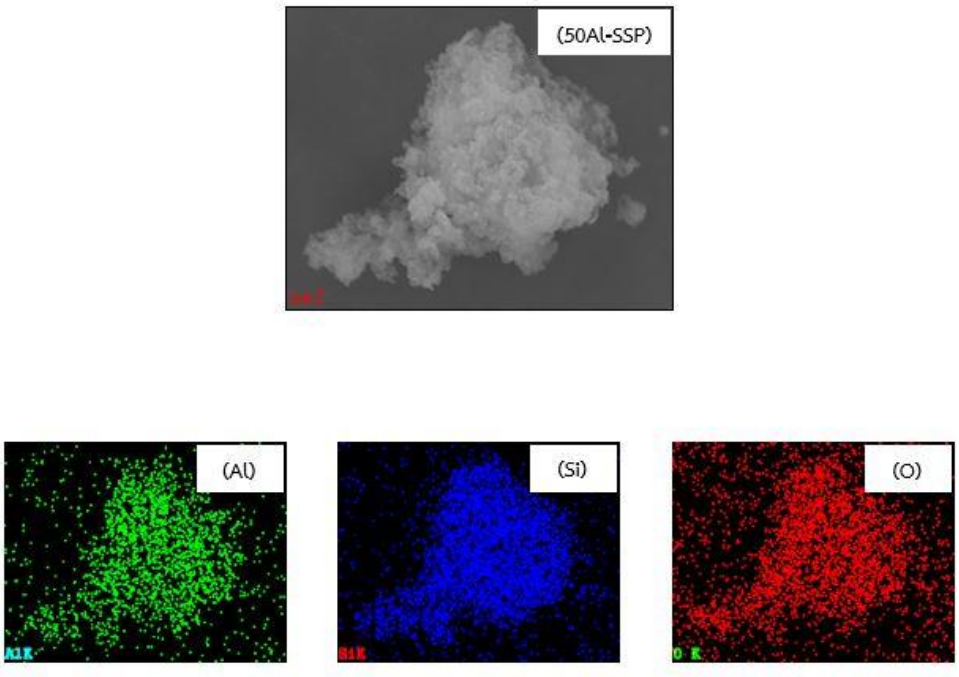

Figure 4.9 EDX mapping of 50Al-SSP catalyst.

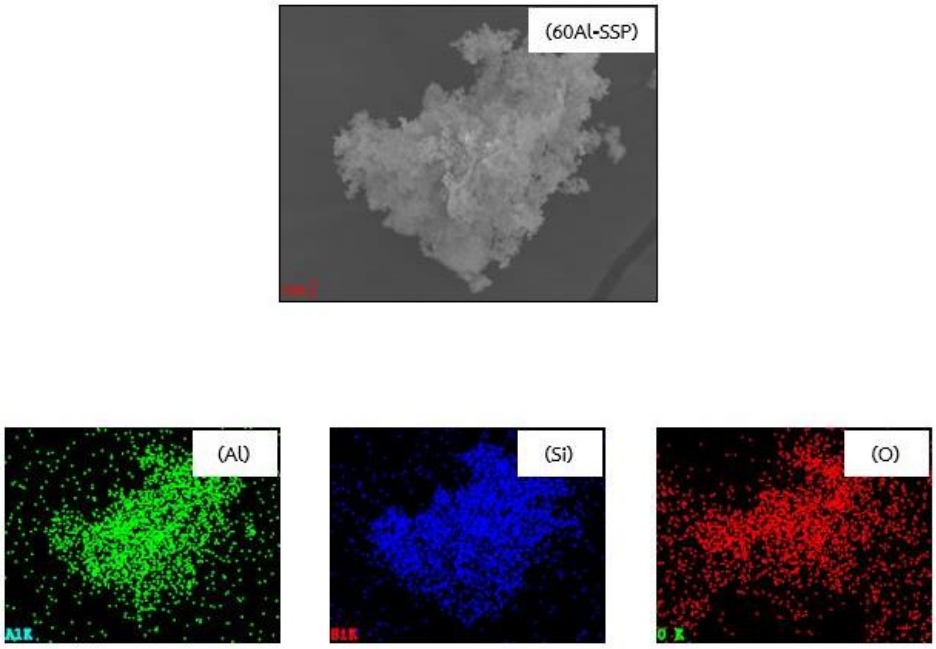

Figure 4.10 EDX mapping of 60Al-SSP catalyst.

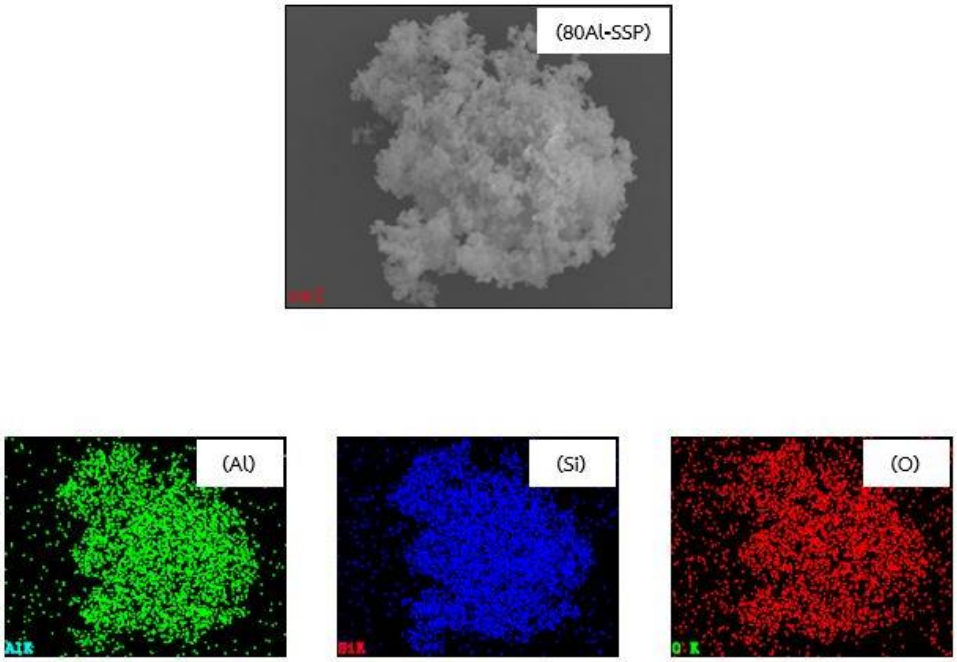

Figure 4.11 EDX mapping of 80Al-SSP catalyst.

4.1.7 Temperature programmed desorption of ammonia (NH_3-TPD)

NH_3-TPD was used to characterize the acidic properties of the alumina-silica composite catalyst. NH_3-TPD profiles of samples are shown in **Figure 4.12**. The profiles and amount of ammonia desorbed from the catalyst can be considered as the number of acid sites and the acid strength distribution on the catalyst, including both Lewis and Brønsted acid sites. Generally, the desorption peaks at low temperature below 250 °C is corresponding to the weak acid sites, whereas those above 400 °C is associated with strong acid sites [34, 39]. As shown in **Figure 4.12**, the Al-SSP composite catalysts have a broad peak at 100-500 °C, due to presence of weak, medium and strong acid sites, while the decrease of the SiO_2/Al_2O_3 leads to the increase of the total acid sites.

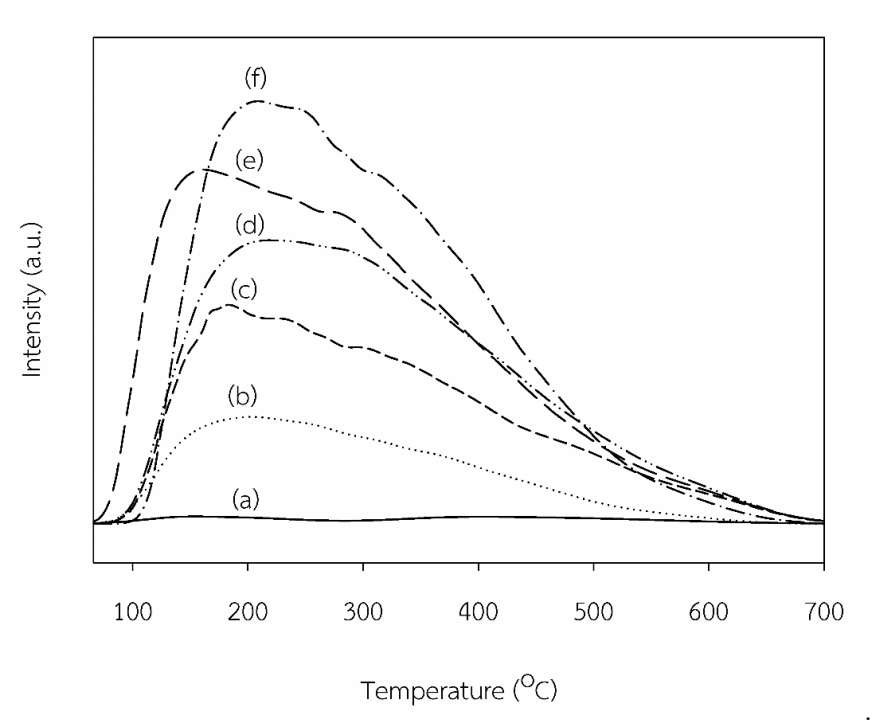

Figure 4.12 NH_3-TPD profiles of samples (a) SSP, (b) 20Al-SSP, (c) 40Al-SSP, (d) 50Al-SSP, (e) 60Al-SSP, (f) 80Al-SSP.

Table 4.3 shows acidic properties of all catalysts. It was found that the amount of the total acid sites on alumina-silica composite catalysts increased with the increasing of alumina content into spherical silica. The number of acid sites on SSP was the lowest when compared with other catalysts. In addition, the 60Al-SSP exhibited the highest total number of acid sites among other composite catalysts. In the previous study, it was reported that the alumina-silica catalyst has both strong Lewis acid sites and significant Brønsted acid sites [3, 6, 15, 16, 20]. Moreover, for ethanol dehydration, alumina-silica catalyst essentially works as a Lewis solid acid more than as a Brønsted solid acid [3, 15, 16, 20]. The trend of total acid site is 80Al-SSP ≈ 60Al-SSP > 50Al-SSP > 40Al-SSP > 20Al-SSP >> SSP, also in agreement with the results of energy dispersive X-ray spectroscopy (EDX) data.

Table 4.3 The amount of acid site of SSP and all alumina-silica composite catalysts.

Catalysts	Number of acid site (μmol NH_3 /g.cat)		
	Weak	Medium-strong	Total
SSP	9	14	23
20Al-SSP	153	90	243
40Al-SSP	271	244	515
50Al-SSP	394	295	689
60Al-SSP	547	359	906
80Al-SSP	532	371	903

4.1.8 Nitrogen physisorption

The N_2 adsorption-desorption isotherms of alumina-silica composite catalysts are shown in **Figure 4.13**. The isotherms of all catalysts could be classified as a type IV according to the IUPAC classification [46], which is typical of mesoporous material. The adsorption in all catalysts at low relative pressure, P/P_0, is due to the monolayer adsorption of nitrogen on the walls of the mesopores.

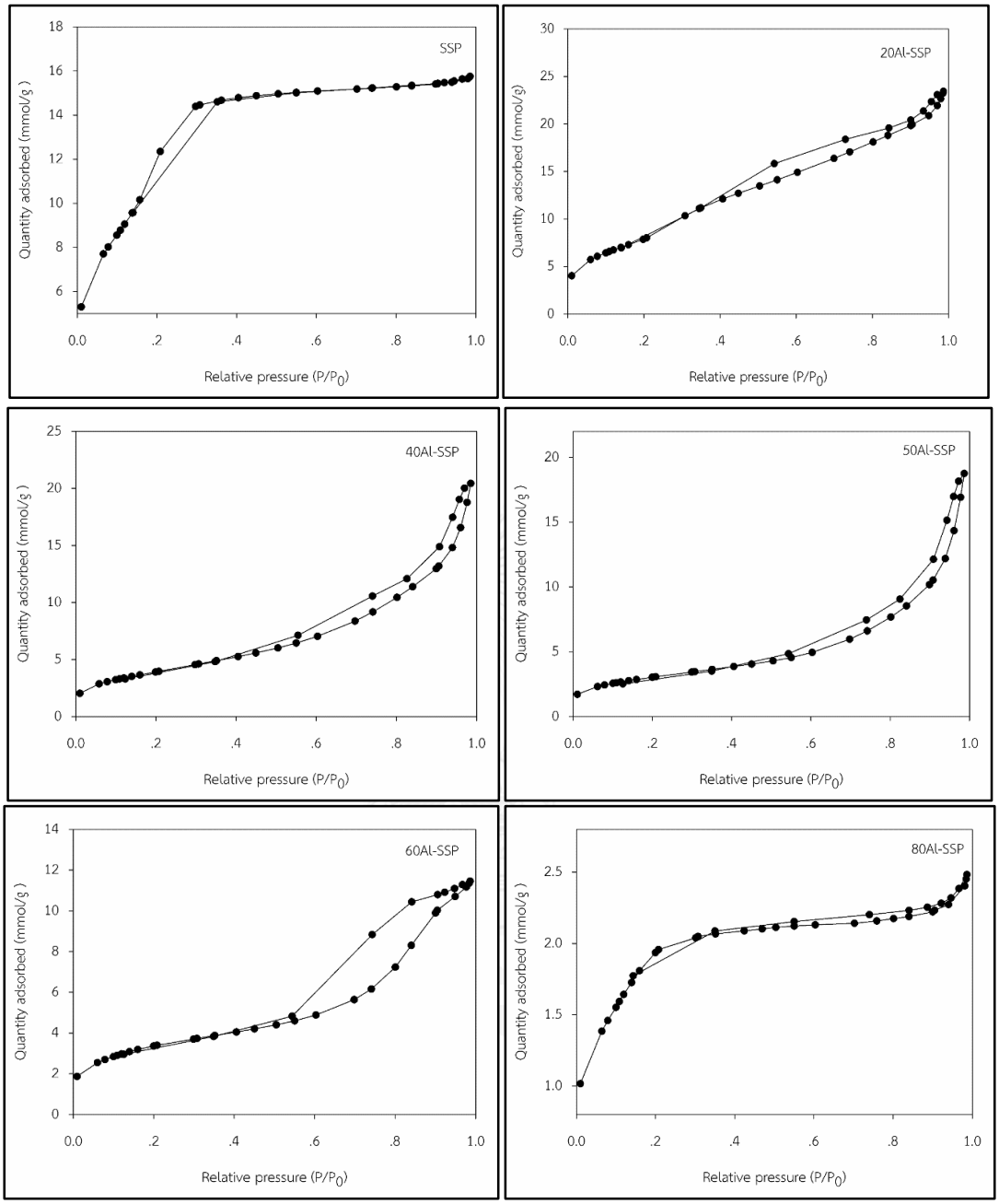

Figure 4.13 Nitrogen adsorption-desorption isotherms of spherical silica particle and all alumina-silica composite catalyst.

The pore size distribution of spherical silica particle and all alumina-silica composite catalysts are presented in **Figure 4.14**. The pore size distributions of SSP, 20Al-SSP and 80Al-SSP show a monomodal distributions with and average pore size diameter of 2.47, 3.34 and 2.99 nm, respectively. While the pore size distributions of

40Al-SSP and 50Al-SSP show a broad pore size distribution in the mesoporous range with an average pore diameter of 6.43 and 8.67 nm, respectively. In addition, the pore size distribution of 60Al-SSP shows good homogeneity of the mesopore structure with an average pore diameter of 5.61 nm.

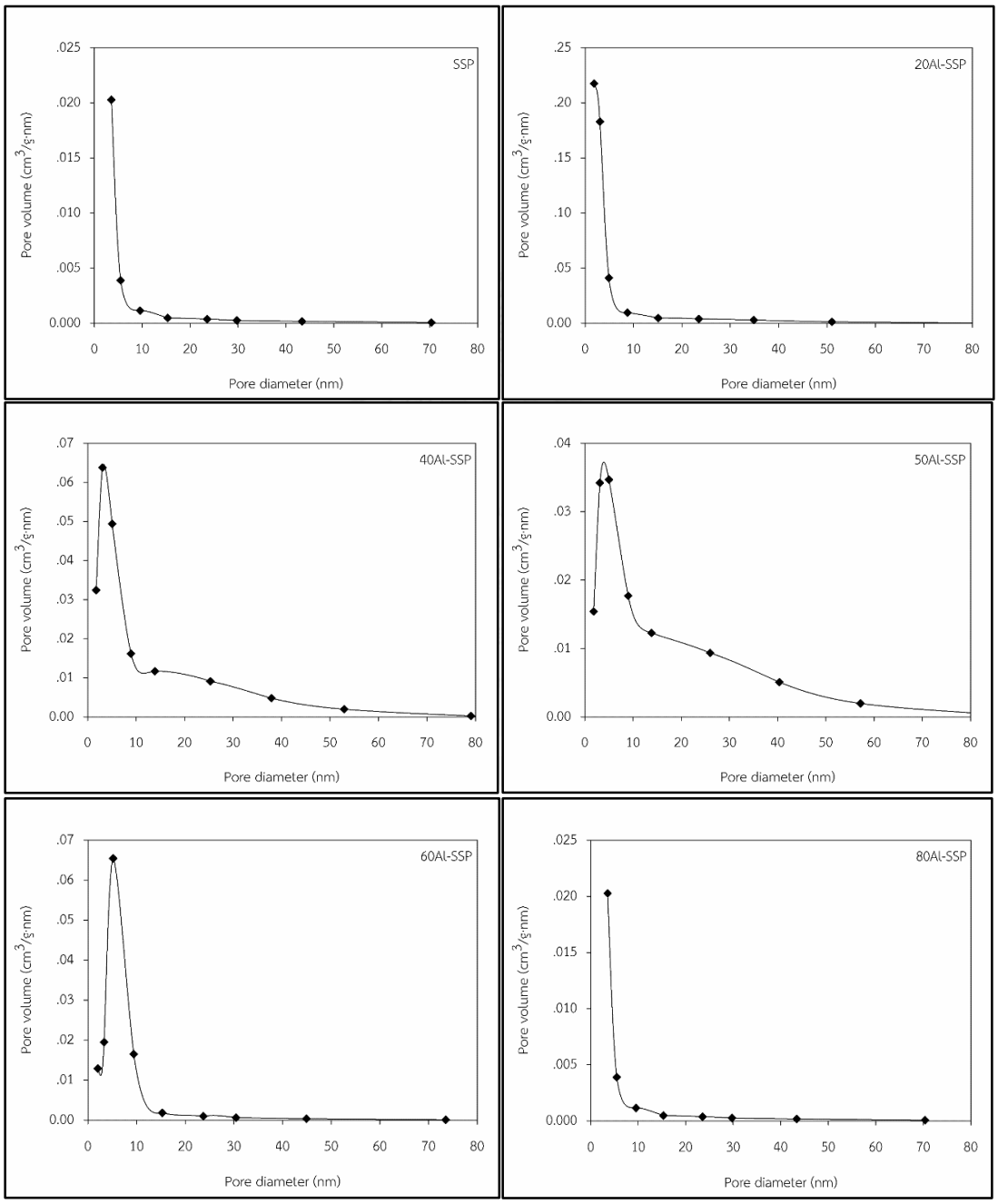

Figure 4.14 Pore size distribution of spherical silica particle and all alumina-silica composite catalyst.

Figure 4.15 and **Table 4.4** show BET surface area, pore volume and pore size diameter results for alumina-silica composite catalysts designated as SSP, 20Al-SSP, 40Al-SSP, 50Al-SSP, 60Al-SSP and 80Al-SSP calcined at 700 ºC, the specific surface areas of the pure silica was significantly higher than those of the alumina-silica composite catalysts. The catalysts with higher Al content showed lower surface area that was comparable with this pure silica. Thus, the addition of Al content to spherical silica catalysts resulted in a reduction of its surface area and pore volume. This is because, the alumina coating on silica surface leading to blocking of pores that are illustrated in **Figure 4.16**. As a result, the nitrogen gas adsorption in pore of catalyst does not occur. The average pore size diameter was ranged from 2.47 to 8.67 nm, with size near the boundary of micro and mesopores. Moreover, the average pore volume of 80Al-SSP was the lowest when compared with other catalysts.

Table 4.4 Summary of physicochemical properties of SSP and all alumina-silica composite catalysts.

Catalysts	BET surface area (m^2/g)	Average pore size (nm)	Average pore volume (cm^3/g)
SSP	1075	2.47	0.69
20Al-SSP	652	3.34	0.85
40Al-SSP	322	6.43	0.72
50Al-SSP	247	8.67	0.66
60Al-SSP	276	5.61	0.41
80Al-SSP	164	2.99	0.05

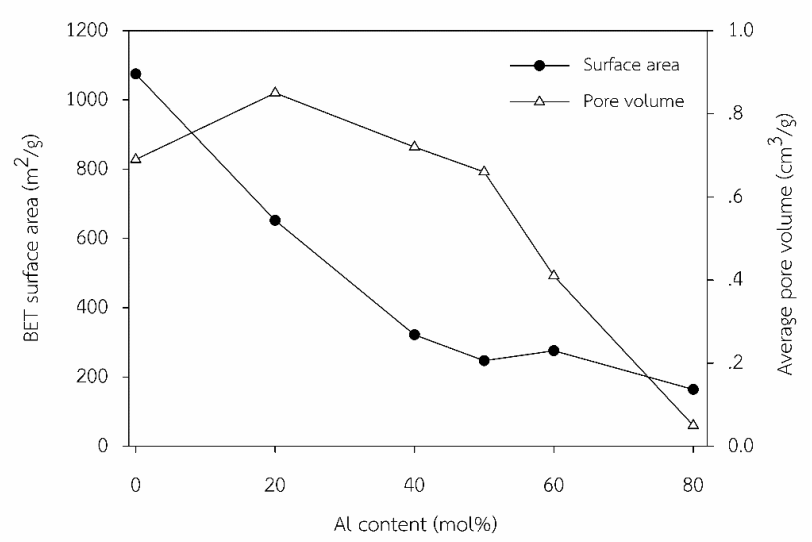

Figure 4.15 Surface area and pore volume of spherical silica particle and all alumina-silica composite catalyst.

Figure 4.16 Alumina coating on silica surface.

4.1.9 Catalytic activity of spherical silica particle and alumina-silica composite catalysts in ethanol dehydration reaction.

Effect of reaction temperature: The effect of reaction temperature on the conversion of ethanol is illustrated in **Figure 4.17**. For all alumina-silica composite catalysts, the conversion of ethanol increases with increasing of reaction temperature. However, the conversion of ethanol at 200 and 250 °C is not significantly different, while the increasing of temperature above 250 °C leads to rapidly enhance the conversion of ethanol. This result indicates that the activity of each catalyst depends on the reaction temperature. However, the activity of SSP catalyst is much lower than

that of all alumina-silica composite catalysts. The selectivity of ethylene and diethyl ether is illustrated in **Figure 4.18** and **Figure 4.19**, respectively. The selectivity of ethylene increased quickly with temperature rising over 250 °C, but the selectivity of diethyl ether is contrary. This is because the ethylene formation reaction and the diethyl ether formation reaction are endothermic and exothermic reaction, respectively. Therefore, at high temperatures favor the ethylene formation reaction, whilst at low temperatures encourage the diethyl ether formation. Moreover, the yield of ethylene is shown that in **Figure 4.21**, indicating that similar trend of conversion of ethanol, nevertheless the yield of diethyl ether increased with increasing the reaction temperature to 300 °C and after that the yield of diethyl ether decreased, which is illustrated in **Figure 4.22**. As the result of the conversion of ethanol at the temperature below 300 °C is low.

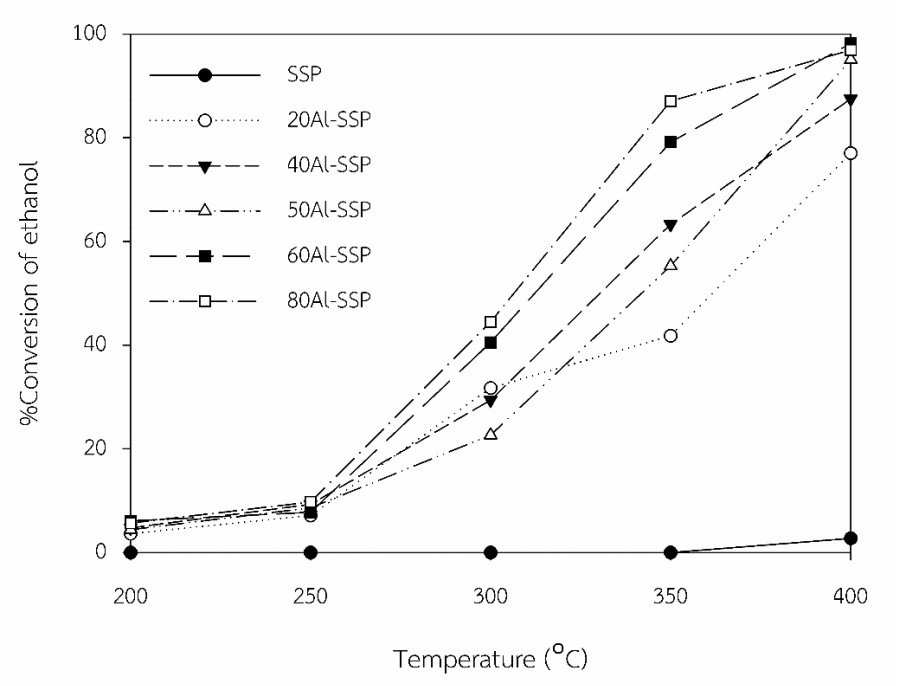

Figure 4.17 Ethanol conversion profiles for spherical silica particle and all alumina-silica composite catalyst in ethanol dehydration reaction at different temperatures.

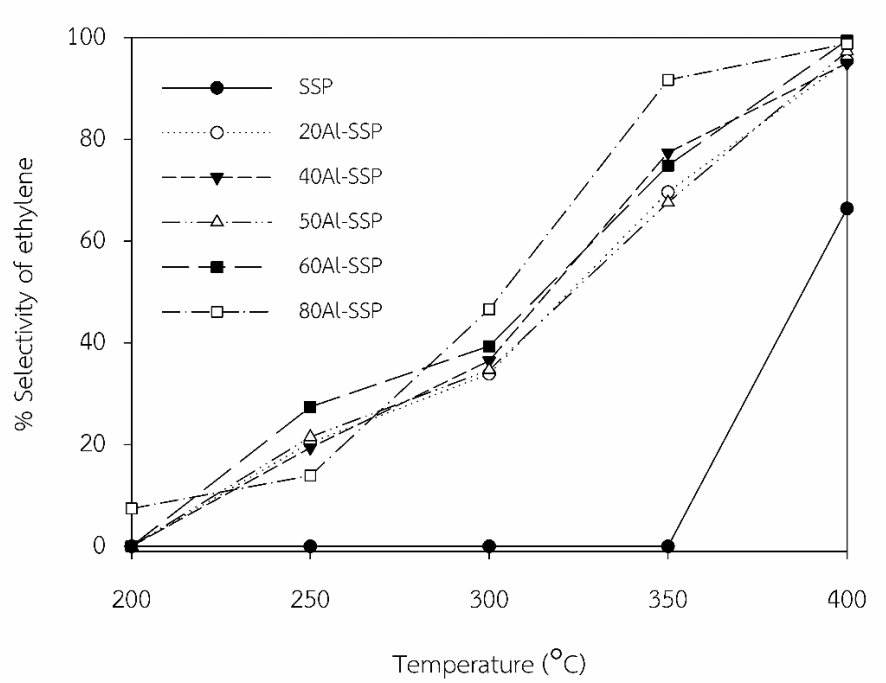

Figure 4.18 Ethylene selectivity profiles for spherical silica particle and all alumina-silica composite catalyst in ethanol dehydration reaction at different temperatures.

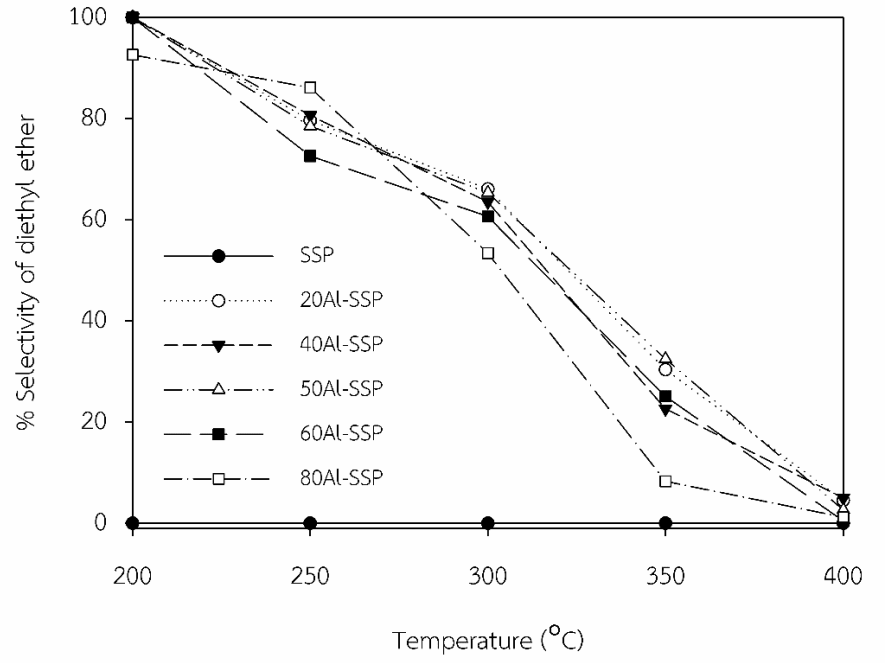

Figure 4.19 Diethyl ether selectivity profiles for spherical silica particle and all alumina-silica composite catalyst in ethanol dehydration reaction at different temperatures.

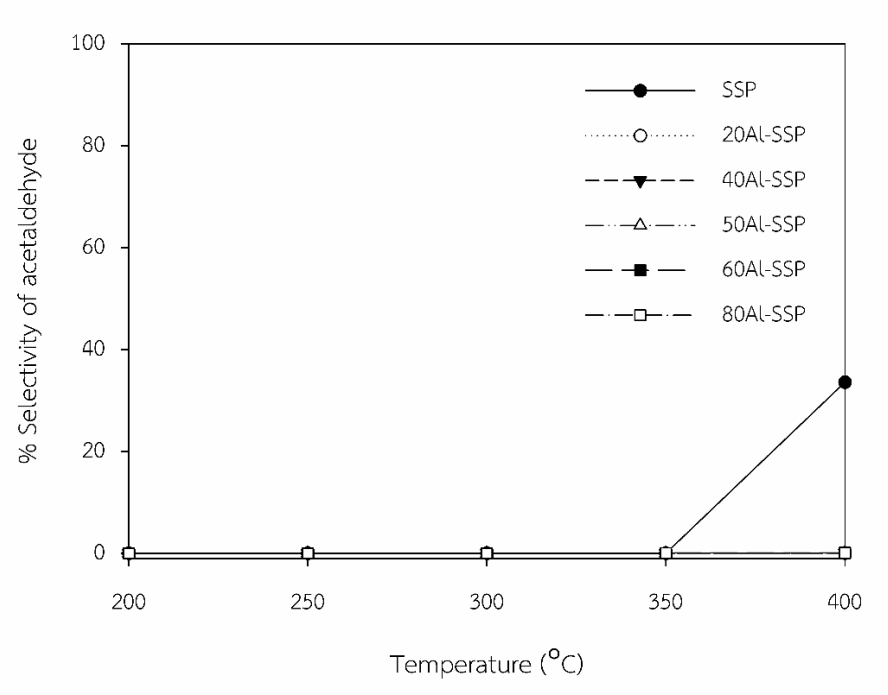

Figure 4.20 Acetaldehyde selectivity profiles for spherical silica particle and all alumina-silica composite catalyst at different temperatures.

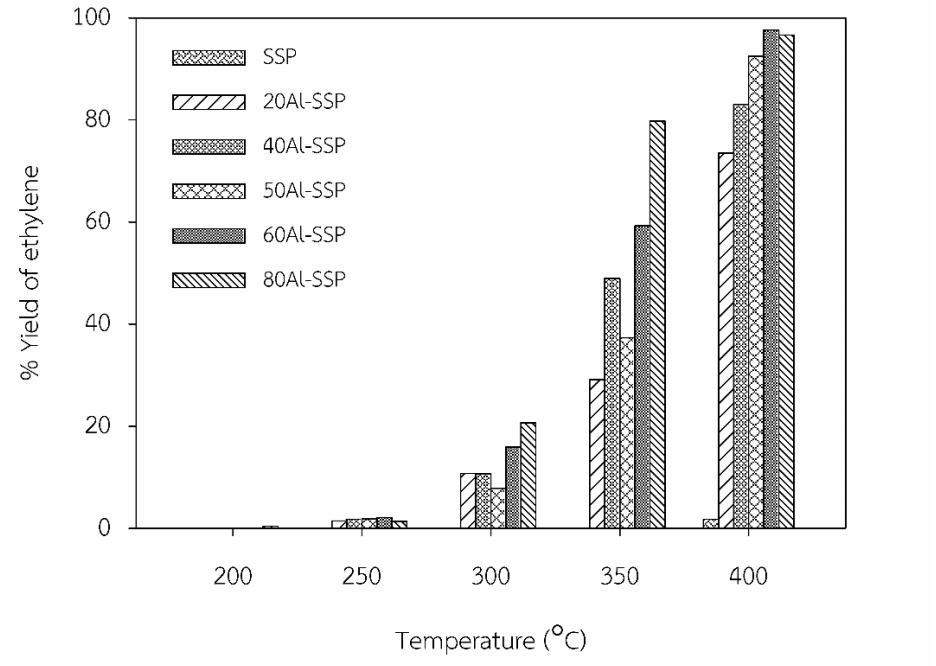

Figure 4.21 Ethylene yield profiles for spherical silica particle and all alumina-silica composite catalyst at different temperatures.

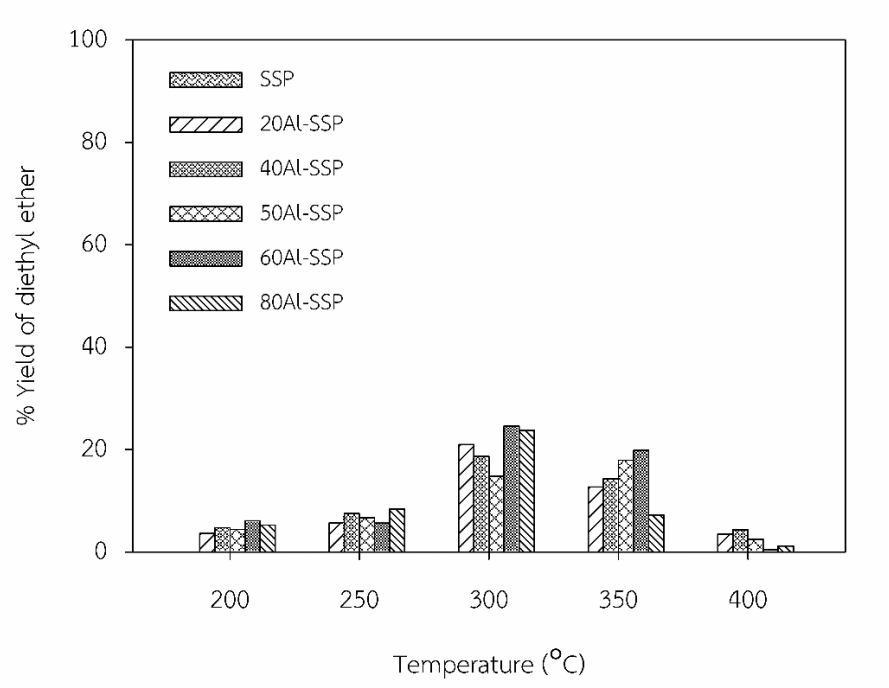

Figure 4.22 Diethyl ether yield profiles for spherical silica particle and all alumina-silica composite catalyst at different temperatures.

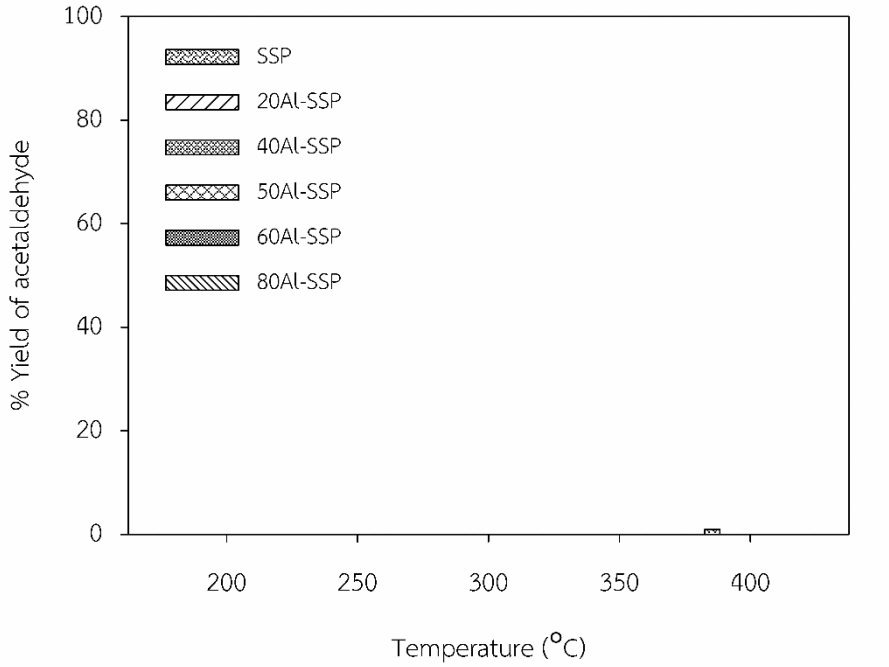

Figure 4.23 Acetaldehyde yield profiles for spherical silica particle and all alumina-silica composite catalyst at different temperatures.

Effect of total acid site: The effect of total acid sites on the ethanol conversion over various catalysts at 400 °C. The results obtained are graphically illustrated in **Figure 4.24.** With the increase in total acid site, conversion of ethanol increased. At this temperature, the highest conversion of ethanol was 98.16% for 60Al-SSP, while the conversion of ethanol was 97.83% for 80Al-SSP. However, the activity of 60Al-SSP and 80Al-SSP is slightly different. The trend of the conversion of ethanol in the experiments performed using the same catalyst weight is 80Al-SSP (97.83%) ≈ 60Al-SSP (98.16%) > 50Al-SSP (95.04%) > 40Al-SSP (87.45%) > 20Al-SSP (77.20%) >> SSP (2.71%). This results agreed with amount of acid sites measured by NH_3-TPD technique in **Table 4.3**, suggesting that the conversion of ethanol depended largely on the amount of total acid sites. The selectivity and yield of ethylene are illustrated in **Figure 4.25** and **Figure 4.26**. The selectivity and yield of ethylene increase with increasing of total acid sites. The lowest selectivity and yield of ethylene was 66.40% and 1.80%, respectively for SSP, while the highest selectivity and yield of ethylene was 99.45% and 97.63%, respectively for 60Al-SSP. In previous studies, they were reported that, alumina-silica presents both strong Lewis acidity and significant Brønsted acidity. Moreover, Lewis acidity is outstanding in the catalysis of alumina-silica catalyst in the dehydration reaction [3, 14, 15] and the increasing of alumina content led to a significant increase of Lewis acid site [24]. Furthermore, the selectivity and yield of diethyl ether are shown in **Figure 4.27** and **Figure 4.28**. The highest selectivity and yield of diethyl ether was 92.59% and 23.74% for 60Al-SSP, respectively. It should be noted that the selectivity and yield of diethyl ether increase with increasing of total acid sites.

The acetaldehyde product is obtained in the catalyst test experiments. As shown in **Figure 4.20** and **Figure 4.23**, the acetaldehyde slightly occurs over SSP catalysts at high temperature. This is because the acetaldehyde formation reaction are

endothermic. Moreover, the dehydrogenation of ethanol to acetaldehyde required basic or redox sites [42].

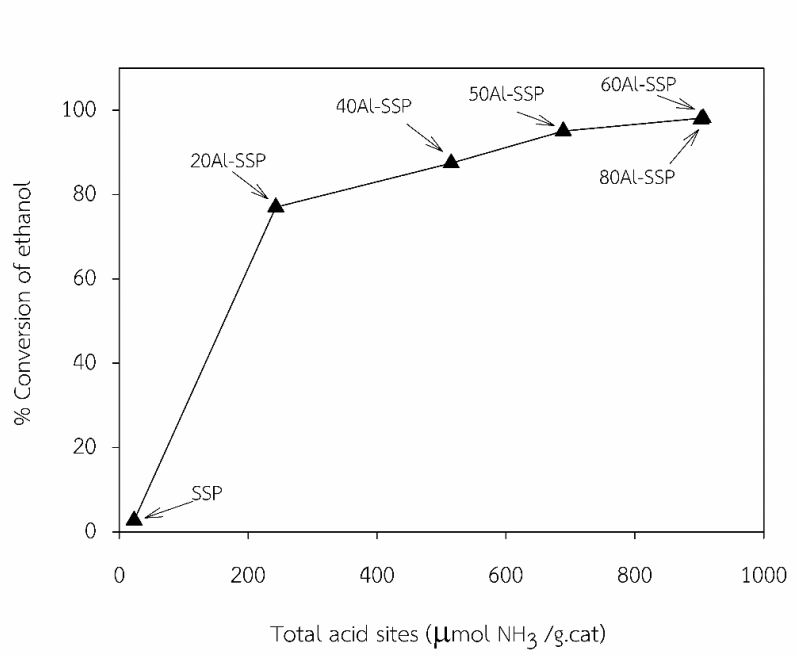

Figure 4.24 Effect of total acid sites on the ethanol conversion over various catalysts (Reaction condition: 400 °C, 99.98 %v/v ethanol, ~ 0.05 g of catalysts).

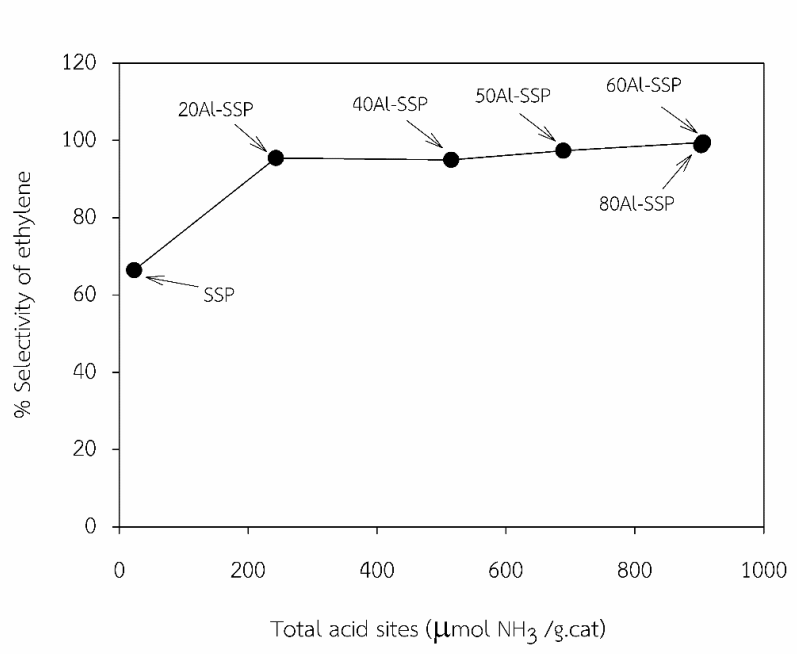

Figure 4.25 Effect of total acid sites on the selectivity of ethylene over various catalysts (Reaction condition: 400 °C, 99.98 %v/v ethanol, ~ 0.05 g of catalysts).

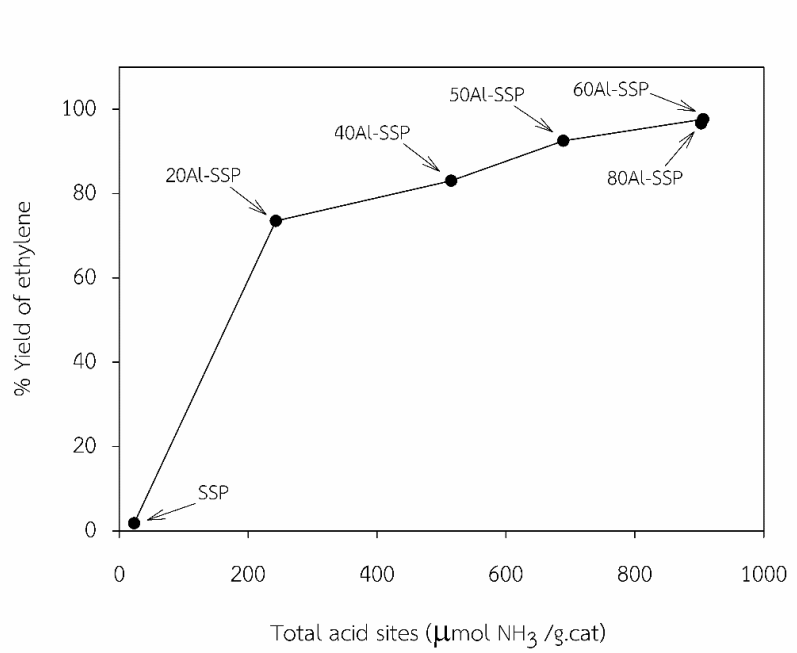

Figure 4.26 Effect of total acid sites on the yield of ethylene over various catalysts (Reaction condition: 400 ºC, 99.98 %v/v ethanol, ~ 0.05 g of catalysts).

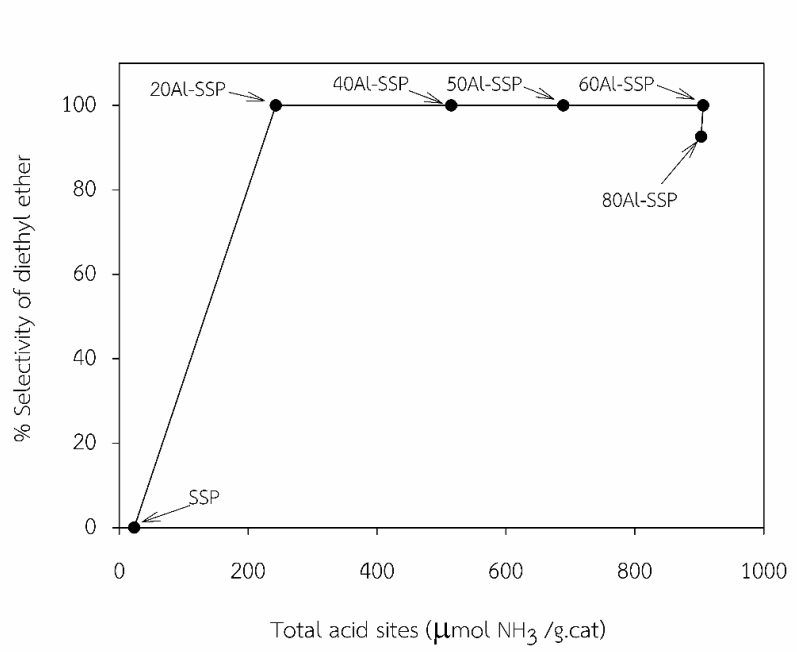

Figure 4.27 Effect of total acid sites on the selectivity of diethyl ether over various catalysts (Reaction condition: 200 ºC, 99.98 %v/v ethanol, ~ 0.05 g of catalysts).

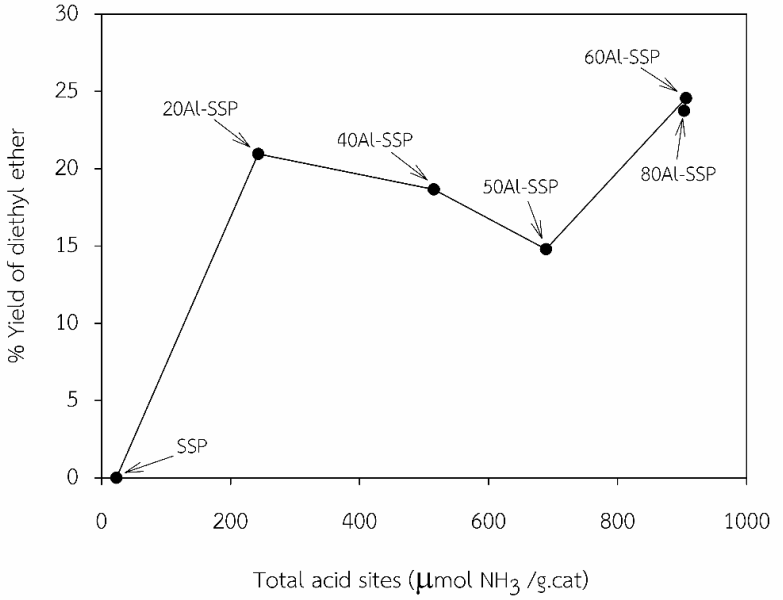

Figure 4.28 Effect of total acid sites on the yield of diethyl ether over various catalysts (Reaction condition: 300 ºC, 99.98 %v/v ethanol, ~ 0.05 g of catalysts).

Effect of surface area: The ethanol conversion activity expressed in terms of the temperature required to obtain 50% conversion, is not correlated with the surface area of alumina silica composite catalysts, but that is correlated with the total acid sites, which is shown in **Figure 4.29**. With increasing total acid sites of alumina silica composite catalysts, the required temperature to reach 50% conversion of ethanol is found to decrease from 360 ºC to 305 ºC due to the increased number of total acid sites, which are active for ethanol dehydration. These results also suggest that a high yield of ethylene can be obtained at high temperature on high acidity of alumina silica composite catalysts.

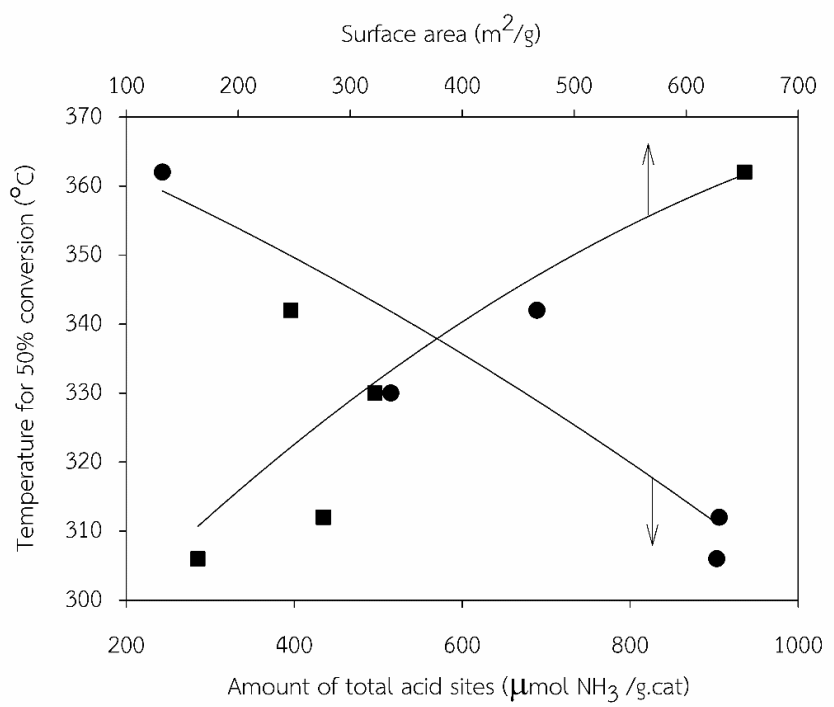

Figure 4.29 Correlation of surface area and amount of total acid sites with the catalytic activity of ethanol dehydration to ethylene and diethyl ether on alumina silica composite catalysts at different alumina contents.

4.2 Catalytic activity of 60Al-SSP in ethanol dehydration reaction with different ethanol concentrations.

Effect of reaction temperature: The effect of reaction temperature on the conversion of ethanol, selectivity of ethylene, selectivity of diethyl ether, yield of ethylene and yield of diethyl ether are shown in **Figure 4.30** to **Figure 4.34**. In each run, various ethanol concentrations were used for ethanol dehydration over 60Al-SSP catalyst. The conversion of ethanol, selectivity of ethylene and yield of ethylene increase with the increasing of temperature. At low temperature, the conversion of ethanol slowly increases, while the increasing of temperature above 300 ºC, it leads to quickly enhance the conversion of ethanol. Moreover, the selectivity of diethyl ether decreased with increasing temperature. Besides, acetaldehyde did not occur over 60Al-SSP at all reaction temperatures.

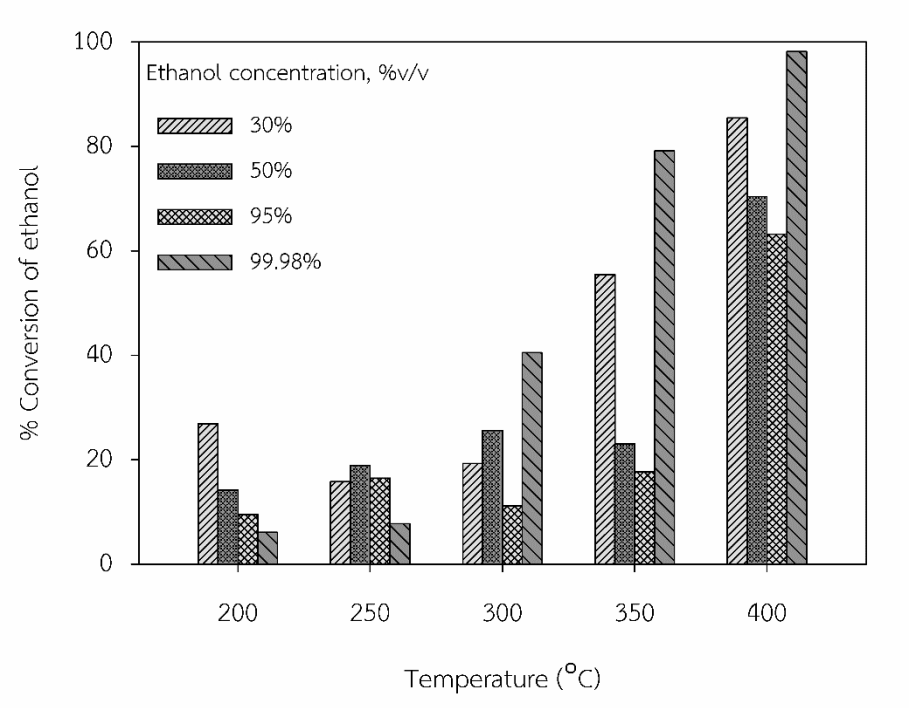

Figure 4.30 Ethanol conversion profiles for 60Al-SSP in ethanol dehydration reaction with different ethanol concentrations.

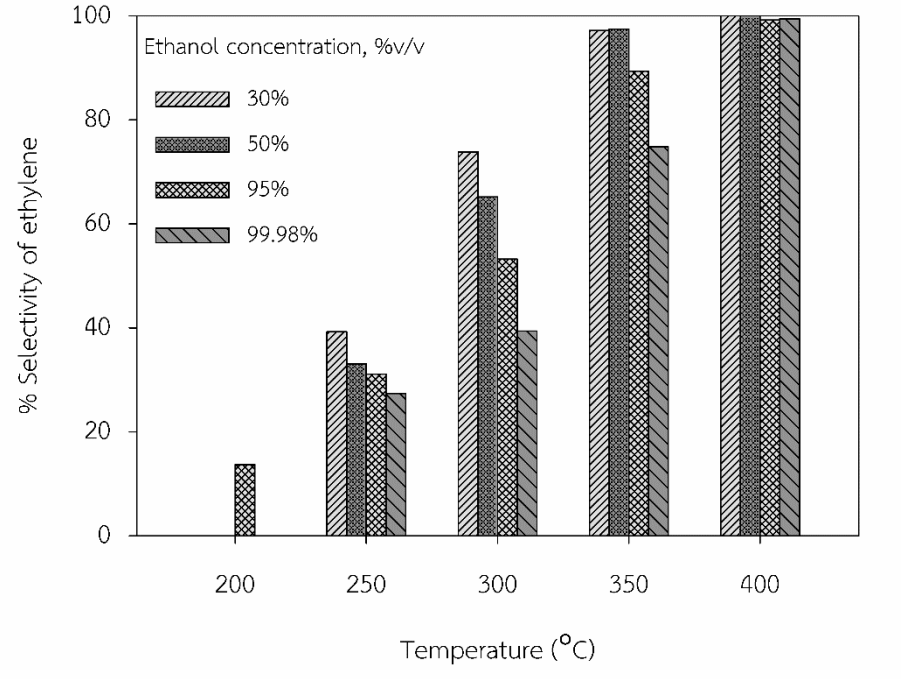

Figure 4.31 Ethylene selectivity profiles for 60Al-SSP in ethanol dehydration reaction with different ethanol concentrations.

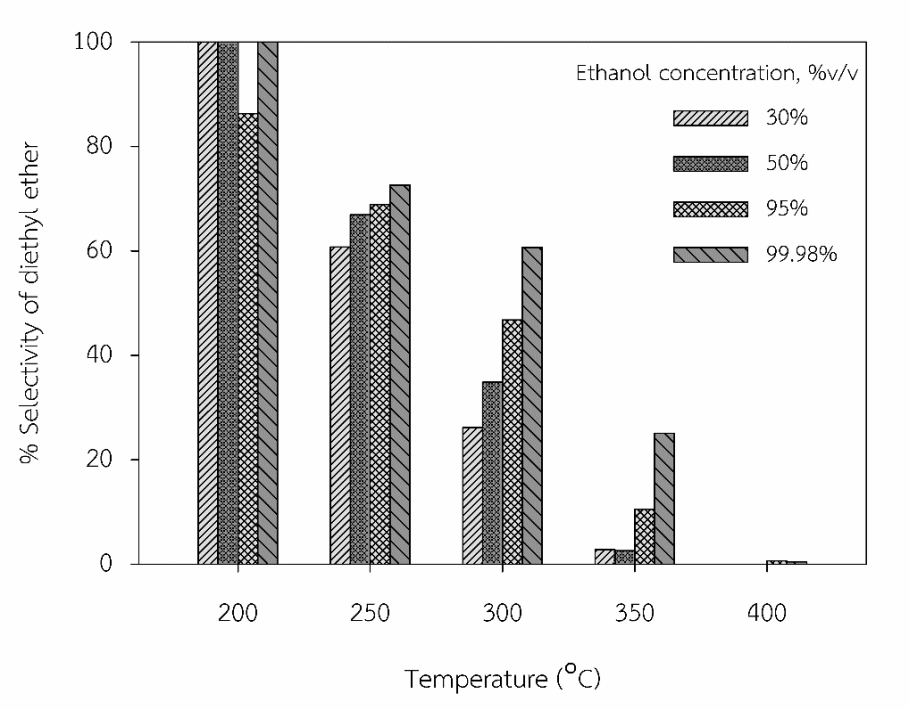

Figure 4.32 Diethyl ether selectivity profiles for 60Al-SSP in ethanol dehydration reaction with different ethanol concentrations.

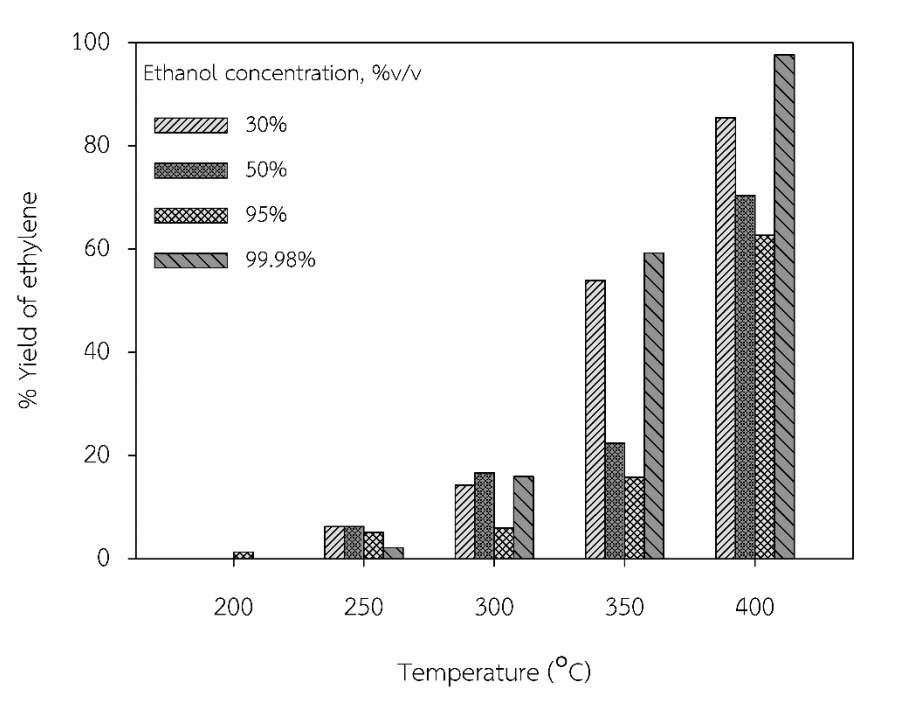

Figure 4.33 Ethylene yield profiles for 60Al-SSP in ethanol dehydration reaction with different ethanol concentrations.

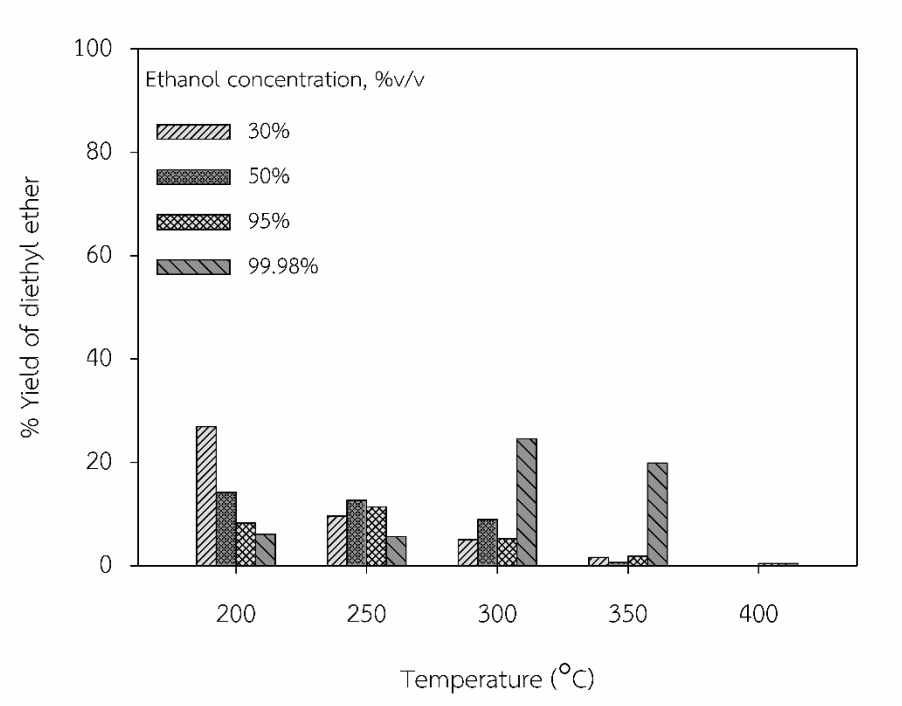

Figure 4.34 Diethyl ether yield profiles for 60Al-SSP in ethanol dehydration reaction with different ethanol concentration.

Effect of ethanol concentrations or water contents: The effects of ethanol concentration (30%v/v, 50%v/v, 95%v/v and 99.98%v/v) on the conversion of ethanol and yield of ethylene over 60Al-SSP are shown in **Figure 4.30** and **Figure 4.33**, respectively. At temperature below 300 °C. The conversion of ethanol and yield of ethylene are not significantly different, while at temperatures above 300 °C, it shows that increasing of water contents in reactant leads to increasing of ethanol conversion and ethylene yield. However, it remains below the ethanol conversion and ethylene yield of pure ethanol. This is because not only the steam (water) at high temperature can convert Brønsted acid sites to Lewis acid sites [18, 47-49], but also the steam (water) was inhibitor that simply blocked adsorption sites on the γ-Al_2O_3 [5, 17]. The comparison between pure ethanol and bioethanol seems to be that the use of pure ethanol is not affected by steam (water). Therefore, the ethanol conversion and yield of ethylene of pure ethanol higher than that of bioethanol. Moreover, the selectivity

of ethylene is shown in **Figure 4.3 1**. The result indicates that the steam (water) can convert Brønsted acid sites to Lewis acid sites because higher selectivity of ethylene occurred at higher water content. Moreover, at low ethanol concentration, it gave high ethylene selectivity because the weak associatively adsorbed ethanol to react with ethoxy groups was low [16]. However as seem from **Figure 4.3 2**, the selectivity of diethyl ether is contrary. In **Figure 4.34**, it shows that the yield of diethyl ether is very low. However, the effect of water could be removed at high temperature [5].

4.3 Investigation of time on stream (TOS) test of 60Al-SSP in ethanol dehydration reaction with pure ethanol and 50 percent volume of ethanol.

The catalytic performance versus time on stream over 60Al-SSP catalyst for the dehydration of 50 %v/v and 99.98%v/v is illustrated in **Figure 4.35** to **Figure 4.37.** The conversion and the ethylene yield of pure ethanol keep constant during 10 hours, while the conversion and the ethylene yield of bioethanol increase from the beginning of the reaction. This is because the Lewis acid sites generation from Brønsted acid sites increase with the increasing of reaction time under high temperature. The conversion of pure ethanol and bioethanol at 10 hours are 99.02% and 96.48%, respectively. The ethylene yield of pure ethanol and bioethanol are 98.63% and 95.97%, respectively. Moreover, the selectivity of ethylene with using pure ethanol and bioethanol are slightly different.

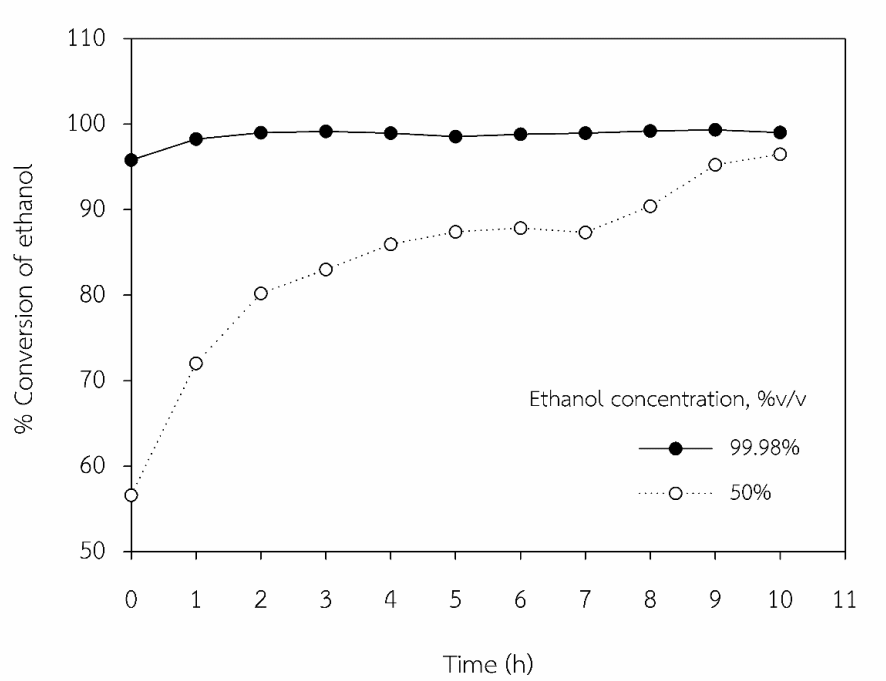

Figure 4.35 Ethanol conversion profiles of 60Al-SSP catalyst for TOS at 400 °C.

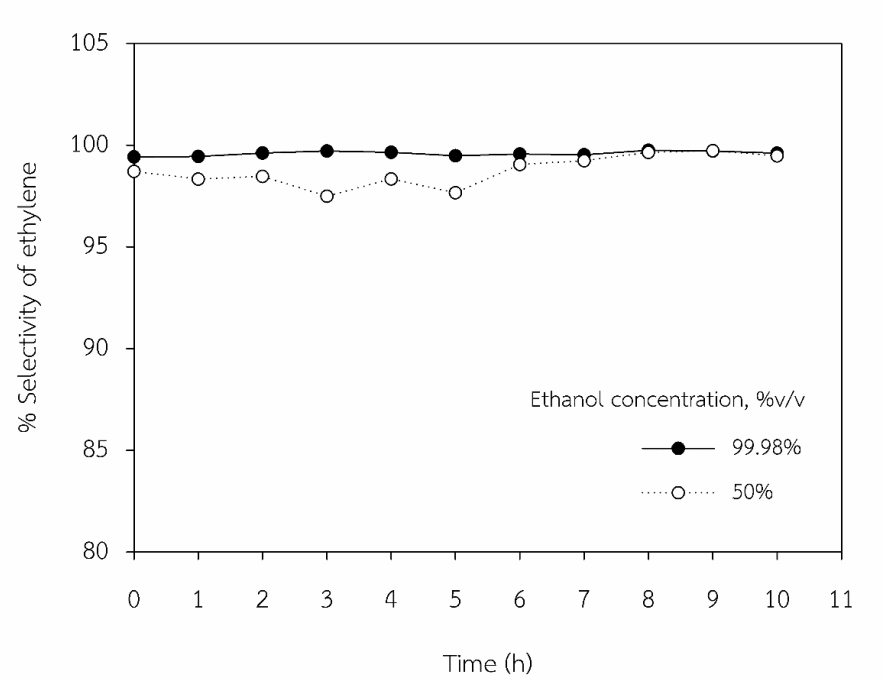

Figure 4.36 Ethylene selectivity profiles of 60Al-SSP catalyst for TOS at 400 °C.

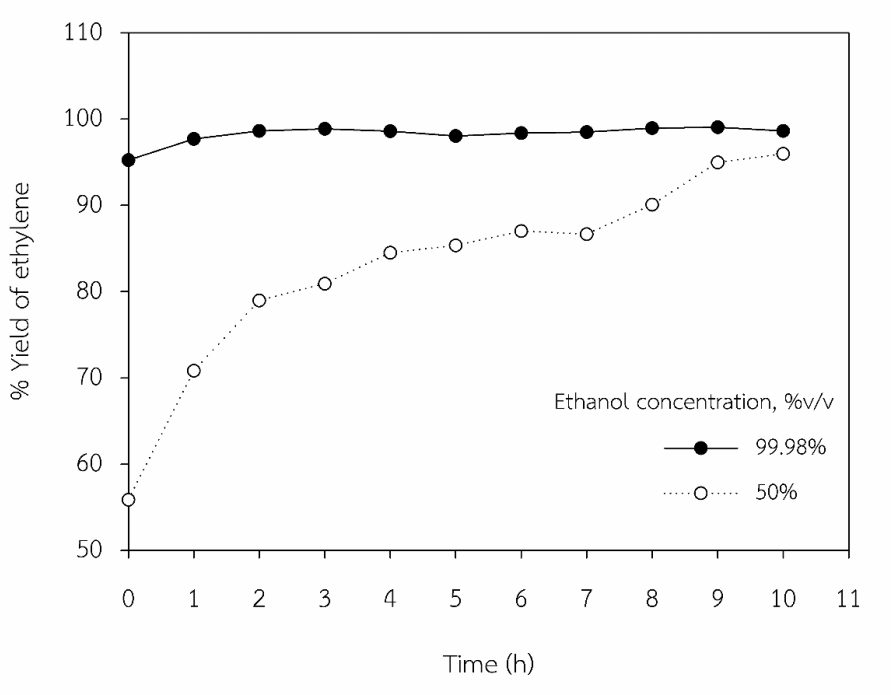

Figure 4.37 Ethylene yield profiles of 60Al-SSP catalyst for TOS at 400 °C.

The amount of coke deposition on catalyst after reaction was determined by thermal gravimetric analysis. The TGA curves of spent catalyst (60Al-SSP) for time on stream (TOS) at 400 °C with 10 hours is shown in **Figure 4.38**. It was observed that the weight loss of catalyst with using pure ethanol and bioethanol are 15% and 12%, respectively. This result suggests that the coke formation on catalyst with using bioethanol is lower than the coke formation on catalyst with using pure ethanol. This is because the ethylene is easy to polymerize on strong Brønsted acid sites of catalyst. The polyethylene can deposits on the catalyst [50]. Meanwhile, the steam (water) at high temperature can convert Brønsted acid sites to Lewis acid sites leading to lower weight loss on catalyst with using bioethanol.

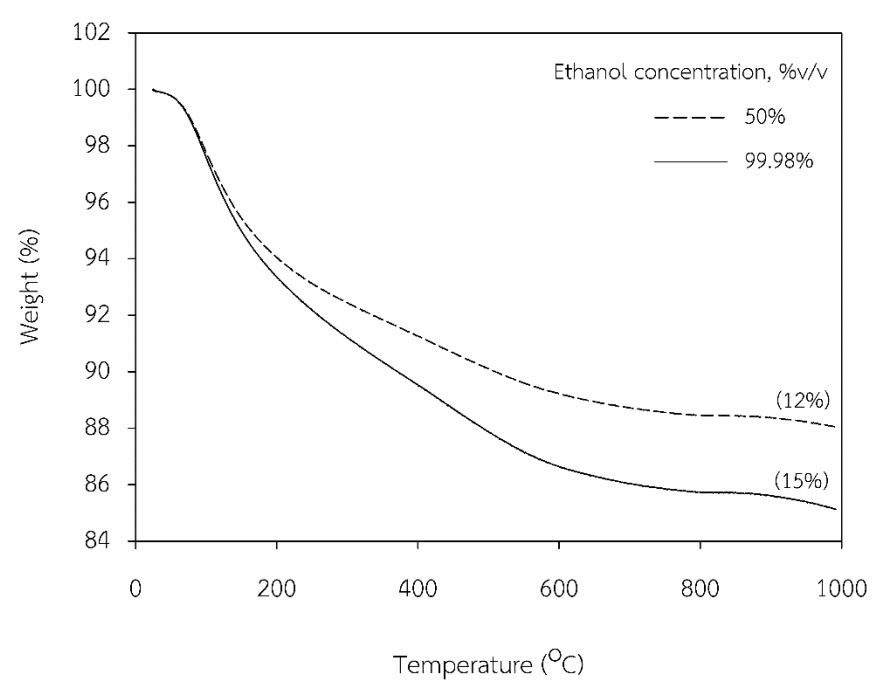

Figure 4.38 Thermal gravimetric analysis curves of spent catalyst (60Al-SSP) for time on stream (TOS) at 400 °C with 10 h.

CHAPTER V
CONCLUSIONS AND RECOMMENDATIONS

Dehydration of ethanol over spherical silica particle and all alumina-silica composite catalysts prepared by modified sol gel method and optimization of ethanol concentration were investigated in this works. In this chapter, we explained about conclusions of the experimental results in section 5.1. Moreover, the recommendation for forward study mentioned in the section 5.2.

5.1 Conclusions

The conclusions of this works can be summarized as follows:

1. The 60Al-SSP composite catalyst exhibited excellent conversion of ethanol and selectivity of ethylene for ethanol dehydration (at high temperature, i.e. 400 °C). This is because, it has the highest amount of total acid sites that it active for this reaction.

2. The effect of ethanol concentration or water content on 60Al-SSP composite catalyst was analyzed via ethanol dehydration. The best yield of ethylene was up to 97.62% over 60Al-SSP composite catalyst at the reaction temperature of 400 °C with using pure ethanol as the reactant. Moreover, the selectivity of ethylene increase with increasing the ethanol concentration, while the selectivity of DEE increase with decreasing the ethanol concentration.

3. The analyzes of coke decompositions over spent catalyst (60Al-SSP) indicated that 60Al-SSP composite catalyst with using bioethanol as the reactant contained less coke decomposition than 60Al-SSP composite catalyst with using pure ethanol as the reactant.

5.2 Recommendations

For the further study;

1. Types of acid, both Lewis and Brønsted acid sites, should be measured by using the pyridine FTIR method.
2. The stability of alumina silica composite catalysts with various alumina content should be investigated.
3. The metals should be impregnated onto the alumina silica composite catalyst for improvement the catalytic performance at low temperature.

REFERENCES

[1] Zhang, M. and Yu, Y. Dehydration of ethanol to ethylene. Industrial & Engineering Chemistry Research 52(28) (2013): 9505-9514.

[2] Fan, D., Dai, D.-J., and Wu, H.-S. Ethylene formation by catalytic dehydration of ethanol with industrial considerations. Materials 6(1) (2012): 101-115.

[3] Phung, T.K., Proietti Hernández, L., Lagazzo, A., and Busca, G. Dehydration of ethanol over zeolites, silica alumina and alumina: Lewis acidity, Brønsted acidity and confinement effects. Applied Catalysis A: General 493 (2015): 77-89.

[4] Zhang, X., Wang, R., Yang, X., and Zhang, F. Comparison of four catalysts in the catalytic dehydration of ethanol to ethylene. Microporous and Mesoporous Materials 116(1-3) (2008): 210-215.

[5] Chen, G., Li, S., Jiao, F., and Yuan, Q. Catalytic dehydration of bioethanol to ethylene over TiO_2/γ-Al_2O_3 catalysts in microchannel reactors. Catalysis Today 125(1-2) (2007): 111-119.

[6] Daniell, W., Schubert, U., Glöckler, R., Meyer, A., Noweck, K., and Knözinger, H. Enhanced surface acidity in mixed alumina–silicas: a low-temperature FTIR study. Applied Catalysis A: General 196(2) (2000): 247-260.

[7] Pines, H. and Haag, W.O. Alumina: catalyst and support. I. alumina, its intrinsic acidity and catalytic activity1. Journal of the American Chemical Society 82(10) (1960): 2471-2483.

[8] Decyk, P., et al. Physicochemical and catalytic properties of iron-doped silica—the effect of preparation and pretreatment methods. Journal of Catalysis 219(1) (2003): 146-155.

[9] Liu, S., et al. The influence of the alcohol concentration on the structural ordering of mesoporous silica: cosurfactant versus cosolvent. The Journal of Physical Chemistry B 107(38) (2003): 10405-10411.

[10] Pieta, I., Ishaq, M., Wells, R., and Anderson, J. Quantitative determination of acid sites on silica–alumina. Applied Catalysis A: General 390(1) (2010): 127-134.

[11] Berteau, P., Ruwet, M., and Delmon, B. 1-butanol Dehydration on aluminas and modified aluminas-evolution of activity and selectivity. Acta Chimica Hungarica 124(1) (1987): 25-33.

[12] Brey, W.S. and Krieger, K. The surface area and catalytic activity of aluminum oxide. Journal of the American Chemical Society 71(11) (1949): 3637-3641.

[13] G., L. and Wade, J. Organic Chemistry, ed. Fifth. New Jersey: Prentice-Hall, 2003.

[14] Phung, T.K. and Busca, G. Diethyl ether cracking and ethanol dehydration: Acid catalysis and reaction paths. Chemical Engineering Journal 272 (2015): 92-101.

[15] Phung, T.K. and Busca, G. Ethanol dehydration on silica-aluminas: Active sites and ethylene/diethyl ether selectivities. Catalysis Communications 68 (2015): 110-115.

[16] Phung, T.K., Lagazzo, A., Rivero Crespo, M.Á., Sánchez Escribano, V., and Busca, G. A study of commercial transition aluminas and of their catalytic activity in the dehydration of ethanol. Journal of Catalysis 311 (2014): 102-113.

[17] DeWilde, J.F., Chiang, H., Hickman, D.A., Ho, C.R., and Bhan, A. Kinetics and mechanism of ethanol dehydration on γ-Al_2O_3: The critical role of dimer inhibition. ACS Catalysis 3(4) (2013): 798-807.

[18] Ong, L.H., Dömök, M., Olindo, R., van Veen, A.C., and Lercher, J.A. Dealumination of HZSM-5 via steam-treatment. Microporous and Mesoporous Materials 164 (2012): 9-20.

[19] Shirai, T., Watanabe, H., Fuji, M., and Takahashi, M. Structural properties and surface characteristics on aluminum oxide powders. Ann Rep Ceram Res Lab Nagoya Inst Technol 9 (2009): 23-31.

[20] Busca, G. The surface of transitional aluminas: A critical review. Catalysis Today 226 (2014): 2-13.

[21] Jetsadanurak, T. Carbon dioxide hydrogenation over alumina-silica composite-supported cobalt catalyst. Chemical Engineering Chulalongkorn University, 2010.

[22] Kaur, M., Sharma, S., and Bedi, P.M. Silica supported Brönsted acids as catalyst in organic transformations: A comprehensive review. Chinese Journal of Catalysis 36(4) (2015): 520-549.

[23] Lebedev, O.I., Van Tendeloo, G., Collart, O., Cool, P., and Vansant, E.F. Structure and microstructure of nanoscale mesoporous silica spheres. Solid state sciences 6(5) (2004): 489-498.

[24] Li, X., Xia, Q., Peng, K., Liu, X., Essayem, N., and Wang, Y. High yield production of HMF from carbohydrates over silica–alumina composite catalysts. Catalysis Science & Technology 6(20) (2016): 7586-7596.

[25] Pilliar, R.M. Solegel surface modification of biomaterials. Surface Coating and Modification of Metallic Biomaterials. 2015.

[26] Somiya, S. Handbook of advanced ceramics: materials, applications, processing, and properties. Academic Press, 2013.

[27] Argyle, M.D. and Bartholomew, C.H. Heterogeneous catalyst deactivation and regeneration: A review. Catalysts 5(1) (2015): 145-269.

[28] Mattos, L.V., Jacobs, G., Davis, B.H., and Noronha, F.b.B. Production of hydrogen from ethanol: review of reaction mechanism and catalyst deactivation. Chemical reviews 112(7) (2012): 4094-4123.

[29] Zaki, T. Catalytic dehydration of ethanol using transition metal oxide catalysts. J Colloid Interface Sci 284(2) (2005): 606-13.

[30] Takahara, I., Saito, M., Inaba, M., and Murata, K. Dehydration of ethanol into ethylene over solid acid catalysts. Catalysis Letters 105(3-4) (2005): 249-252.

[31] Varisli, D., Dogu, T., and Dogu, G. Ethylene and diethyl-ether production by dehydration reaction of ethanol over different heteropolyacid catalysts. Chemical Engineering Science 62(18-20) (2007): 5349-5352.

[32] Xiao, Y., Li, X., Yuan, Z., Li, J., and Chen, Y. Catalytic dehydration of ethanol to ethylene on TiO_2/4A Zeolite composite catalysts. Catalysis Letters 130(3-4) (2009): 308-311.

[33] Ramesh, K., Zheng, J.E., Ling, E.G.Y., Han, Y.-F., and Borgna, A. Synthesis, characterization, and catalytic activity of uniformly crystalline $LaPO_4$ nanofiber catalysts for ethanol dehydration. The Journal of Physical Chemistry C 113(37) (2009): 16530-16537.

[34] Chen, Y., et al. Dehydration reaction of bio-ethanol to ethylene over modified SAPO catalysts. Journal of Industrial and Engineering Chemistry 16(5) (2010): 717-722.

[35] Zotov, R.A., Molchanov, V.V., Volodin, A.M., and Bedilo, A.F. Characterization of the active sites on the surface of Al_2O_3 ethanol dehydration catalysts by EPR using spin probes. Journal of Catalysis 278(1) (2011): 71-77.

[36] Wang, F., Luo, M., Xiao, W., Cheng, X., and Long, Y. Coking behavior of a submicron MFI catalyst during ethanol dehydration to ethylene in a pilot-scale fixed-bed reactor. Applied Catalysis A: General 393(1-2) (2011): 161-170.

[37] León, M., Díaz, E., and Ordóñez, S. Ethanol catalytic condensation over Mg–Al mixed oxides derived from hydrotalcites. Catalysis Today 164(1) (2011): 436-442.

[38] Bedia, J., Barrionuevo, R., Rodríguez-Mirasol, J., and Cordero, T. Ethanol dehydration to ethylene on acid carbon catalysts. Applied Catalysis B: Environmental 103(3-4) (2011): 302-310.

[39] Bokade, V.V. and Yadav, G.D. Heteropolyacid supported on montmorillonite catalyst for dehydration of dilute bio-ethanol. Applied Clay Science 53(2) (2011): 263-271.

[40] Han, Y., Lu, C., Xu, D., Zhang, Y., Hu, Y., and Huang, H. Molybdenum oxide modified HZSM-5 catalyst: Surface acidity and catalytic performance for the dehydration of aqueous ethanol. Applied Catalysis A: General 396(1-2) (2011): 8-13.

[41] Matachowski, L., Zimowska, M., Mucha, D., and Machej, T. Ecofriendly production of ethylene by dehydration of ethanol over $Ag_3PW_{12}O_{40}$ salt in nitrogen and air atmospheres. Applied Catalysis B: Environmental 123-124 (2012): 448-456.

[42] Mahmoud, H.R. Highly dispersed $Cr_2O_3–ZrO_2$ binary oxide nanomaterials as novel catalysts for ethanol conversion. Journal of Molecular Catalysis A: Chemical 392 (2014): 216-222.

[43] Phung, T.K., Proietti Hernández, L., and Busca, G. Conversion of ethanol over transition metal oxide catalysts: Effect of tungsta addition on catalytic

behaviour of titania and zirconia. Applied Catalysis A: General 489 (2015): 180-187.

[44] Padmaja, P., Pillai, P.K., Warrier, K., and Padmanabhan, M. Adsorption isotherm and pore characteristics of nano alumina derived from sol-gel boehmite. Journal of Porous Materials 11(3) (2004): 147-155.

[45] Aravind, P., Mukundan, P., Pillai, P.K., and Warrier, K. Mesoporous silica–alumina aerogels with high thermal pore stability through hybrid sol–gel route followed by subcritical drying. Microporous and Mesoporous Materials 96(1) (2006): 14-20.

[46] Rouquerol, J., Rouquerol, F., Llewellyn, P., Maurin, G., and Sing, K.S. Adsorption by powders and porous solids: principles, methodology and applications. Academic press, 2013.

[47] Gounder, R. Hydrophobic microporous and mesoporous oxides as Brønsted and Lewis acid catalysts for biomass conversion in liquid water. Catalysis Science & Technology 4(9) (2014): 2877-2886.

[48] Ravenelle, R.M., et al. Stability of zeolites in hot liquid water. The Journal of Physical Chemistry C 114(46) (2010): 19582-19595.

[49] Sheng, Q., Ling, K., Li, Z., and Zhao, L. Effect of steam treatment on catalytic performance of HZSM-5 catalyst for ethanol dehydration to ethylene. Fuel Processing Technology 110 (2013): 73-78.

[50] Bi, J., Guo, X., Liu, M., and Wang, X. High effective dehydration of bio-ethanol into ethylene over nanoscale HZSM-5 zeolite catalysts. Catalysis Today 149(1) (2010): 143-147.

APPENDIX

APPANDIX A

CALCULATION FOR CATALYST PREPARATION

Calculation of alumina-silica composite catalysts

- Ratio for spherical silica particle synthesis.

Molar ratio	1TEOS	: 0.3 CTAB	: 11 NH_3	: 58 Ethanol	: 144 H_2O
Mw	208.3	364.46	17	46	18
g	208.33	109.34	187	2668	2592
/100	2.1	1.1	1.9	26.7	25.9

Example: The 60 mol% of alumina in alumina-silica composite catalyst (60Al-SSP) was prepared by modified sol-gel method

Basis: 40% Si = 1 mole TEOS

60% Al = 1.5 mole

60Al: 40Si

Using Si 1 mole = TEOS 2.1 g

Using Al 1.5 mole = $Al(NO_3)_3.9H_2O$ 5.63 g

APPANDIX B

CALCULATION FOR ACID SITES OF CATALYSTS

Calculation of acidity

The acidity was measured by NH_3-TPD, it can be calculated from NH_3-TPD profile as follows;

$$\text{Acidity of catalysts} = \frac{\text{mol of } NH_3 \text{ desorption}}{\text{amount of dry catalyst}} \text{---------- equation (B.1)}$$

To Calculate mole of NH_3 desorption from the calibration curve of NH_3 as follow:

NH_3 desorption (mole) = 0.0003 x A

Where, A is area under peak of the NH_3-TPD profile.

And then, we denote amount of dry catalyst as B (g.). So the equation (B.1) can be take place as equation (B.2)

$$\text{Acidity of catalysts} = \frac{0.003 \times A}{B} \text{---------- equation (B.2)}$$

APPANDIX C

CALIBRATION CURVE

Calibration curves were used calculation mole of ethanol, ethylene, DEE and acetaldehyde as shown in **Figure C.1 - C.4**. The concentration of these were analyzed by the gas chromatography Shimadzu model 14A, capillary column DB-5 of flame ionization detector (FID). The conditions uses in GC are presented in **Table C.1**

Table C.1 Conditions use in GC-14A.

Parameters	Condition
Width	5
Slope	100
Drift	0
Min.area	300
T.DBL	1000
Stop time	8 min
Atten	2
Speed	3
Method	Normalization
SPL.WT	100
IS.WT	1

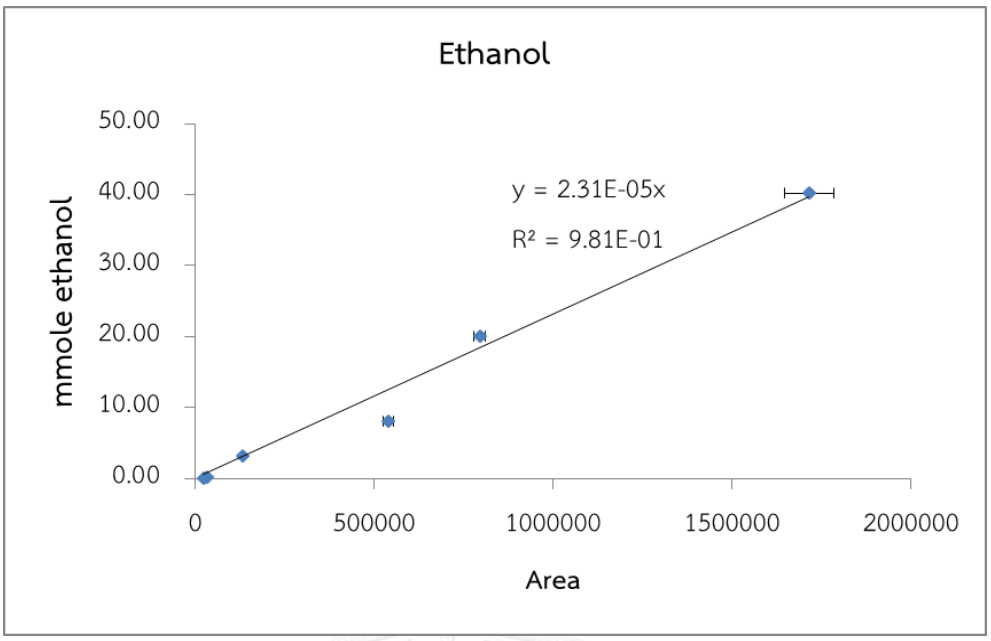

Figure C.1 The calibration curve of ethanol.

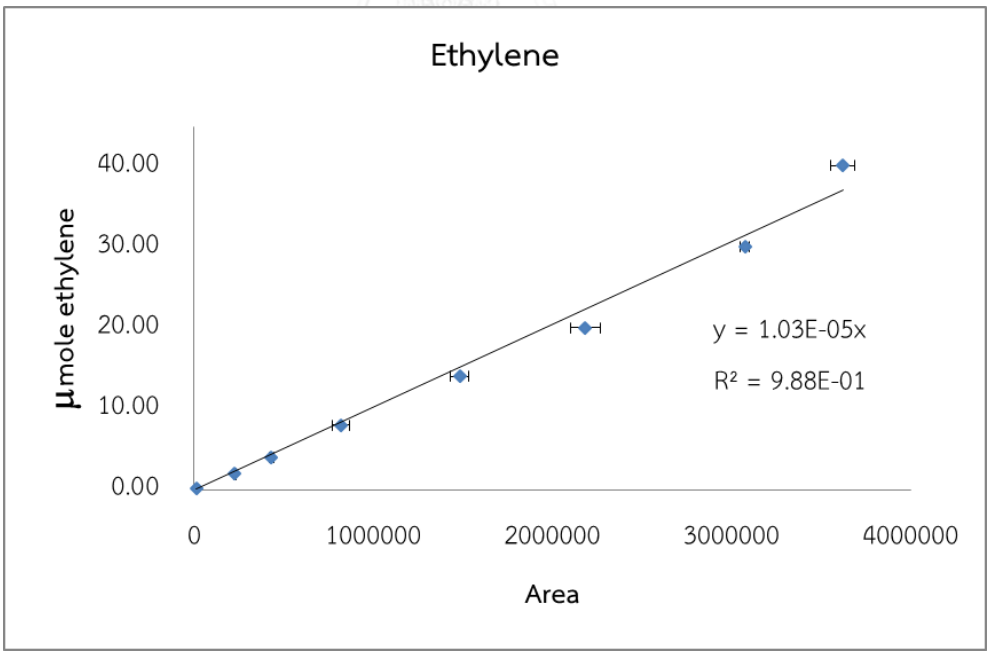

Figure C.2 The calibration curve of ethylene.

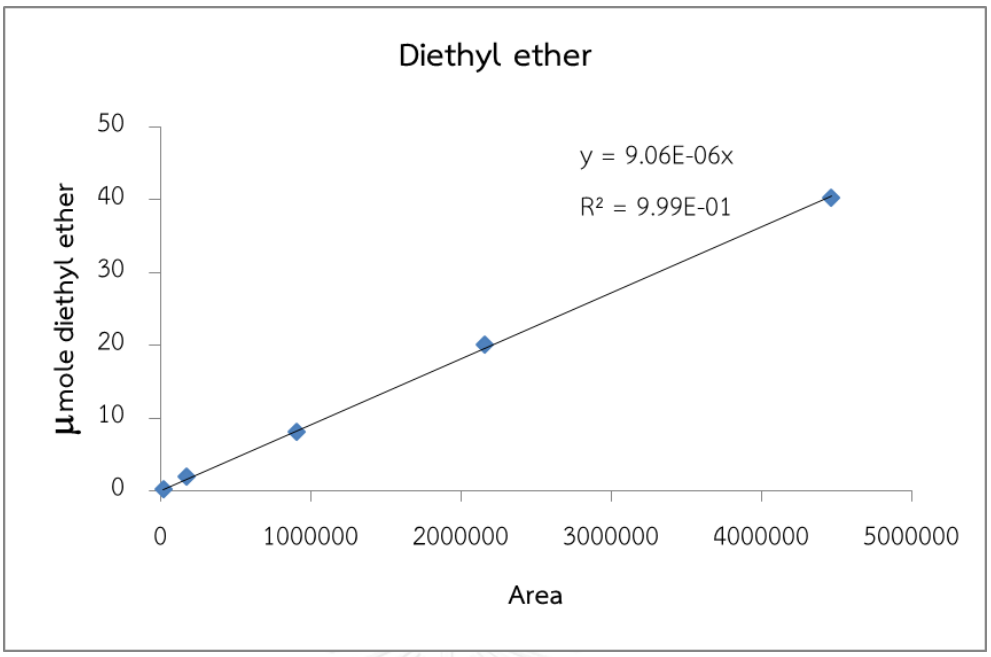

Figure C.3 The calibration curve of DEE.

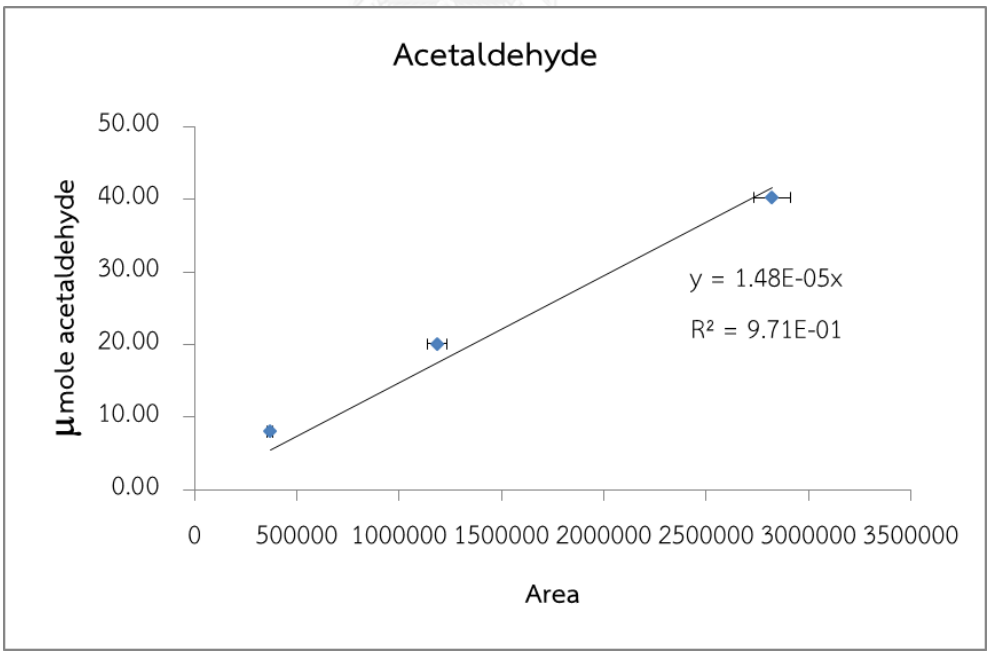

Figure C.4 The calibration curve of acetaldehyde.

APPANDIX D

CONVERSION, SELECTIVITY AND YIELD

The catalytic performance for the ethanol conversion was evaluated in term of activity for ethanol conversion.

C.1 Ethanol conversion

$$\text{Ethanol conversion (\%)} = \frac{(\text{mole of ethanol in feed} - \text{mole of ethanol in product}) \times 100}{\text{mole of ethanol in feed}}$$

Products selectivity are defined as moles of products converted with respect to product in out of reaction as follows:

C.2 Selectivity of product

$$\text{Ethylene selectivity (\%)} = \frac{\text{mole of ethylene in product} \times 100}{\text{mole of total products}}$$

$$\text{Diethyl ether selectivity (\%)} = \frac{\text{mole of DEE in product} \times 100}{\text{mole of total products}}$$

$$\text{Acetaldehyde selectivity (\%)} = \frac{\text{mole of acetaldehyde in product} \times 100}{\text{mole of total products}}$$

Where: Total product is mole of (Ethylene + DEE + Acetaldehyde).

Products yield was evaluated in term of ethanol conversion and products selectivity

$$\text{Ethylene yield (\%)} = \frac{\text{ethylene selectivity} \times \text{ethanol conversion}}{100}$$

$$\text{DEE yield (\%)} = \frac{\text{DEE selectivity} \times \text{ethanol conversion}}{100}$$

$$\text{Acetaldehyde yield (\%)} = \frac{\text{acetaldehyde selectivity} \times \text{ethanol conversion}}{100}$$

From calibration curve;

Mole of ethanol = (2.31×10^{-5}) x area

Mole of ethylene = (1.03×10^{-5}) x area

Mole of diethyl ether = (9.06×10^{-6}) x area

Mole of acetaldehyde = (1.48×10^{-5}) x area

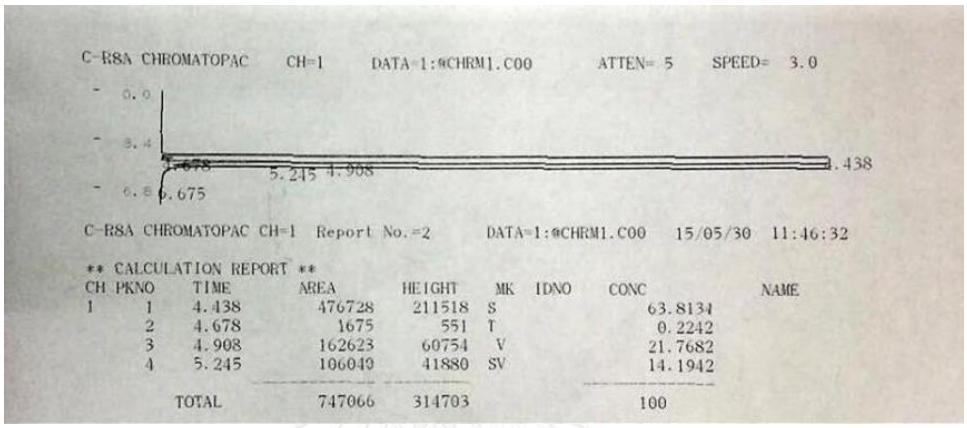

Figure D.1 The GC result

Example;

From **Figure D.1**, the area of reactant and product can be detected by gas chromatography. The peak at 4.438 minute shown area of ethylene, while peak at 4.678, 4.908 and 5.245 minute represented area of acetaldehyde, ethanol and diethyl ether, respectively.

So, mole of ethanol = (2.31×10^{-5}) x 162623

= 3.76 mole

APPANDIX E

LIST OF PUBLICATION

Proceeding

Phairoj Tochaeng and Bunjerd Jongsomjit, “The ethanol dehydration over Al-SSP composite catalysts derived from modified sol-gel method.” Proceeding of the 22nd Regional Symposium on Chemical Engineering: RSCE 2015, Bangkok, Thailand, September 24-25, 2015.

VITA

Mr. Phairoj Tochaeng was born on September 20th, 1990 in Phichit, Thailand. He finished high school from Taphanhin School in 2008, and He received the bachelor's degree of Petrochemicals and Polymeric Materials from the Department of Materials Science and Engineering, Faculty of Engineering and Industrial Technology, Silpakorn University in March 2013. He continued the Master of Engineering in Chemical Engineering, Faculty of Engineering, Chulalongkorn University in October 2013.